Assembly and Function of Photosystem I

in Higher Plants

Dissertation

zur Erlangung des Doktorgrades der Fakultät für Biologie

der Ludwig-Maximilians-Universität München

Department Biologie I, Botanik

vorgelegt von

Katrin Amann

aus Schliersee

Erstgutachter: Prof. R.G. Herrmann
Zweitgutachter: Prof. H.-U. Koop

Datum der mündlichen Prüfung: 20.01.2006

Content

3

Content

Abbreviations

μE	micro-Einstein (1 E = 1 mol of photons)
Å	Ångstrom
A_0	PSI primary electron acceptor composed of chlorophyll a
A_1	PSI secondary electron acceptor composed of phylloquinone
ATP	adenosine 5′-triphosphate
bp	base pairs
BSA	bovine serum albumin
cDNA	complementary DNA
CES	control by epistasy of synthesis
Ci	Curie
cpm	counts per minute
$cytb_6f$	cytochrome b_6f-complex
DNA	deoxyribonucleic acid
dNTPs	deoxynucleoside triphosphates
EDTA	ethylenediaminetetraacetic acid
EGTA	ethylene glycol-bis(2-aminoethylether)-N,N,N',N'-tetraacetic acid
EMS	ethyl methanesulfonate
ESTs	expressed sequence tags
F_A	[4Fe-4S] cluster of the PsaC subunit
F_B	[4Fe-4S] cluster of the PsaC subunit
FTR	ferredoxin-thioredoxin reductase
F_X	interpolypeptide [4Fe-4S] cluster between PsaA and PsaB subunits
g	gravity force, gramme
GTP	guanosine 5′-triphosphate
hcf	high chlorophyll fluorescence
HEPES	N-[2-Hydroxyethyl]piperazine-N'-[2-ethanesulfonic acid]
K	Kelvin
kb	kilobases
kDa	kilodalton
LHCI	chlorophyll-binding PSI light-harvesting complex
Mb	megabases

MES	2-morpholinoethanesulfonic acid
MOPS	3-[N-morpholino]propanesulfonic acid
mRNA	messenger RNA
NADP$^+$	nicotinic adenine dinucleotide phosphate
NPQ	non-photochemical chlorophyll *a* fluorescence quenching
P700	PSI primary electron donor chlorophyll *a*
PAM	pulse amplitude–modulated fluorometer
PC	plastocyanine
PCR	polymerase chain reaction
PEG	polyethylene glycol
PSI	photosystem I
PSII	photosystem II
PVDF	polyvinylidene difluoride
qP	photochemical chlorophyll *a* fluorescence quenching
RF	release factor
RNA	ribonucleic acid
rpm	revolutions per minute
rRNA	ribosomal RNA
RT-PCR	reverse transcription PCR
S	Svedberg unit
SD	standard deviation
SDS	sodium dodecyl sulfate
SDS-PAGE	SDS-polyacrylamide gel electrophoresis
SSLP	simple sequence length polymorphism
Suc	sucrose
T-DNA	transferred DNA
Tricine	N-Tris-(hydroxymethyl)-methylglycine
Tris	Tris-(hydroxymethyl)-aminomethane
tRNA	transfer RNA
Tween	polyoxyethylenesorbitan monolaurate
U	unit, enzyme activity
UTR	untranslated region
v/v	volume per volume

w/v   weight per volume

I. Introduction

1. Oxygenic photosynthesis

The uniting structure of oxygenic photosynthesis is the thylakoid membrane located in the cytosol of cyanobacteria and in photosynthetic plastids of algae and plants. The four major protein complexes of this membrane involved in oxygenic photosynthesis are, in order of the reaction photosystem II (PS-II), the cytochrome b_6f-complex (cytb_6f), photosystem I (PSI-LHCI) and the ATP synthase (CF_0-CF_1). In addition, relatively complex light harvesting assemblies (LHCI and LHCII) are associated to the two photosystems and some smaller proteins and cofactors perform vital electron shunting tasks and the final reduction of $NADP^+$ (Figure 1).
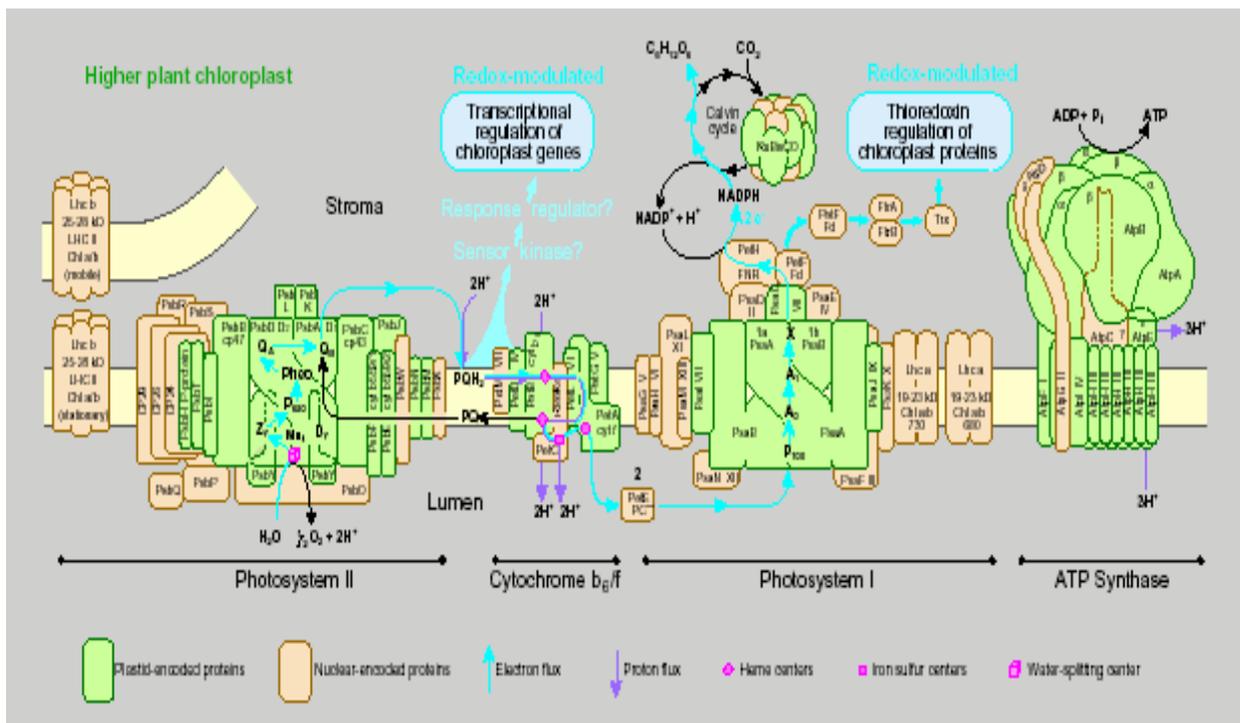
Figure 1: A schematic cut-through diagram of the thylakoid membrane, showing the protein complexes and electron carriers involved, as well as the stoichiometries of protons in oxygenic photosynthesis. Stoichiometries of the reactions indicated refer to the production of a single molecule of O_2 (modified from Herrmann 1996).

The protein complexes involved in oxygenic photosynthesis are not evenly distributed in the thylakoid membrane. The two photosystems are spatially separated. PSI-LHCI is located in stroma lamellae membranes and at the margins of the grana stacks, while PSII to a great extent, is only present in grana stacks (Danielsson *et al.*, 2004). The Cyt*b₆f* is evenly distributed between the two regions (Ganeteg, 2004), whereas the ATP synthase complex is located at fringe regions of grana and in stroma lamella (Jansson *et al.*, 1997). While the structure and function of most of the protein complexes involved in oxygenic photosynthesis are quite well described, the biogenesis and turnover of the different complexes have not been investigated to a comparable degree.

2. Structure and function of higher plant PSI-LHCI

The higher plant PSI complex core is composed of at least 15 different subunits, named alphabetically from PSI-A to PSI-P, excluding PSI-M which, like PSI-X, is exclusively present in cyanobacteria (Inoue *et al.*, 2004). In addition, the light harvesting antenna I (LHCI) that associates to PSI on one side to the complex is composed of at least four different light harvesting proteins, designated Lhca1- Lhca4. Besides the protein subunits there is a relatively large complement of pigments and cofactors, at least 167 chlorophyll molecules, about 27 ß-carotenes, 10 luteins, 6 violaxanthins (Ganeteg, 2004) and 3 iron sulphur clusters (4Fe-4S). Taken together the findings make PSI to one of the largest protein complexes found in nature, with a molecular mass of 567 kilo Dalton (kDa) according to the subunit composition determined from the crystal structure of pea PSI-LHCI (Ben-Shem *et al.*, 2003).
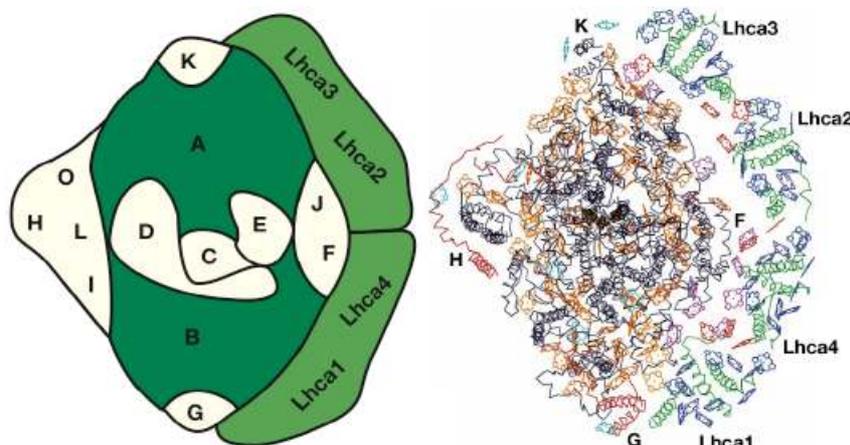
Figure 2: The structure of the entire higher plant PSI-LHCI complex, when viewed from the stromal side of the thylakoid membrane. Left: Model of higher plant PSI-LHCI complex, indicating the assignment/position of all subunits, except of PSI-N. The original model was published in Jensen *et al.* (2003) and modified in accordance to Jensen *et al.* (2004) with regard to PSI-O and the Lhca1-4 assignments in accordance to (Ben-Shem *et al.*, 2003) Right: The crystal structure of PSI-LHCI complex from pea, solved at 4.4 Å resolution, including cofactors and pigments. Subunits similar to cyanobacterial PSI are in black, later additions to the PSI complex are in red and the LHCI proteins are in green. The assignment of Lhca1-4 and the positions of the F, G, H and K subunits are indicated. The chlorophylls are depicted in different colours according to their assigned location and/or putative function: LHCI chlorophylls (blue), energy transfer between LHCI monomers (red), special function in energy migration between LHCI and the RC (magenta), conserved chlorophylls in the RC (yellow), added chlorophylls to the RC (cyan) (Ben-Shem *et al.*, 2003).

The functions of various PSI subunits have been identified (Scheller *et al.*, 2001). The two major subunits, PsaA and PsaB, are plastid-encoded, form the central heterodimer and serve as anchors for binding cofactors necessary for light absorbance and the primary photochemical reactions. PsaA and PsaB bind pairs of the primary electron donor and acceptor chlorophylls, P700 and A_0, respectively, the phylloquinone A_1 and the [4Fe-4S] cluster F_x. The other two [4Fe-4S] clusters (F_A and F_B) are bound to plastid-encoded PsaC and transfer electrons from F_x to ferredoxin. Additional chlorophyll molecules are associated with the core complex and the outer antenna proteins Lhca1 - Lhca4 and involved in light absorbing and energy transfer (Saenger *et al.*, 2002; Golbeck, 2003).

3. Photosystem II, cytochrome b_6f-complex and chloroplast ATP synthase complexes

Besides the crystal structure of pea PSI (Ben-Shem et al., 2003) there are also crystal structures of the cyanobacterial PSII complex (Kamiya and Shen, 2003), the chloroplast PSII (Rhee, 2001), the plant major light-harvesting complex (Liu *et al.*, 2004) and the cytochrome b_6f complex from unicellular algae (Stroebel *et al.*, 2003) and cyanobacteria (Kurisu *et al.*, 2003) available.

Like PSI, PSII is a membrane-spanning, dimeric multisubunit pigment-protein complex. The energy absorbed by the LHCs is transferred to the reaction centres. In a multi-step process, the energy of 4 photons is used to oxidise two molecules of water to molecular oxygen. Based on the results from crystal structure analysis the primary organisation of PSII between cyanobacteria and higher plants is basically conserved, but there are also differences in some peripherical PSII subunits as well as in the antenna and the composition of the water splitting system (Hankamer *et al.*, 2001; Barber and Nield, 2002; Kashino *et al*, 2002).

The cytochrome b_6f complex is a pigment-protein complex which mediates the electron flow between the two photosystems, functions as a plastoquinol-plastocyanin-oxidoreductase and contributes to the formation of a proton gradient used to synthesize ATP, it is also involved in cyclic electron transport around PSI (Clark and Hind, 1983). The data for the cytochrome b_6f complex reveals a dimeric structure and is essentially the same in unicellular algae and cyanobacteria (Strobel *et* al., 2003; Kurisu *et al*., 2003).

Electron transport from water to $NADP^+$ is light-dependent and generates a transmembrane electrochemical proton gradient used by the chloroplast ATP synthase for photophosphorylation (Evron *et al*., 2000). The ATP synthase complex is conserved between eubacteria, mitochondria and plastids with regard to structure, composition and basic organisation (Strotmann *et al*., 1998; Groth and Pohl, 2001).

4. Biogenesis of thylakoid membrane protein complexes

The biogenesis of thylakoid membrane protein complexes can be divided into 3 major processes: (1) The biogenesis of the constituent subunits and their cofactors and pigments, (2) their translocation and insertion to the thylakoid membrane, and (3) their assembly into an oligomeric protein complex . Each of these major processes rests on multiple steps, is subject to multiple control mechanisms, and requires many proteins besides the subunits comprising the photosynthetic apparatus (Wollman *et al.*, 1999). One last major process vital to the biogenesis that the 3 major processes do not cover is proteolytic processing or degradation. It is an important participant at every step of biogenesis as well as when the complexes exceed their lifespan or become damaged (Adam, 2000; Adam and Ostersetzer, 2001). The biogenesis of protein complexes are complicated by the fact that the genes encoding subunits and auxiliary proteins are not located in the same genome. While some reside in the chloroplast genome (the plastome), others are located in the nuclear genome (Scheller *et al.*, 2001). This distribution is due to the origin of the chloroplast. More than 1.5 billion years ago the chloroplast as it is known today was a free living cyanobacterium and while some genes have been translocated to the nuclear genome; some remained in the plastome. There could be a number of reasons why it is not possible to move all the genes of the plastome to the nucleus (Martin & Herrmann, 1998).

Nevertheless, the fact remains that the genes are distributed and the cells spend a great deal of effort and energy to regulate and operate the two genome systems (Leister and Schneider, 2003).

During evolution of photoautotrophic eukaryotes, the nucleus has gained a dominant role in the coordination of the integrated genetic system of the cell consisting of three specifically coevolved genetic compartments. The photosynthetic machinery is encoded by the chloroplast and nuclear genomes. Therefore, biosynthesis and assembly of stochiometric amounts of subunits as well as association of the proteins with corresponding cofactors need to be managed and precisely regulated.

5. PSI-LHCI biogenesis

The biogenesis of the PSI-LHCI complex has only partially been elucidated. The genes responsible for the subunits of the complex, their transcription, the proteins responsible for the transcription and the posttranscriptional processing have been reasonably well described both from the nucleus and the chloroplast. In addition, quite substantial information is also known from translation and translocation of the nuclear encoded proteins. While all these areas are well explored, there are still aspects of the biogenesis left to evaluate.

The assembly of PSI-LHCI starts with the translation and translocation of PSI-B into the thylakoid membrane. The initiation of PSI-B translation, in *Arabidopsis thaliana*, is controlled by at least two nuclear encoded factors, Tab1 and Tab2 (Dauvillee *et al.*, 2003; Stampacchia *et al.*, 1997). In *Chlamydomonas reinhardtii*, the translation of PSI-B initiates a CES controlled translation cascade that so far has shown to include the translation of PSI-A and PSI-C (Wostrikoff *et al.*, 2004). The initiation of PSI-A translation requires the presence of PSI-B and the initiation of PSI-C translation requires the presence of PSI-A (Wostrikoff *et al.*, 2004). The stable accumulation of PSI-A requires both the translation of PSI-B and the stable assembly into the AB core. The latter is achieved by assembly of the two subunits and the insertion of the majority of the chlorophyll *a* and the F_X iron-sulphur cluster (Wollman *et al.*, 1999).

Without the insertion of F_X, the AB core does not accumulate in neither plant nor algae nor cyanobacteria (Golbeck, 2003; Lezhneva and Meurer, 2004). When the AB core has assembled the translation of PSI-C is initiated (Wostrikoff *et al.*, 2004). When PSI-C is translated, it does not associate to the AB core, unless the F_A and F_B iron-sulphur clusters are inserted (Yu *et al.*, 1997).

6. Nuclear control of chloroplast gene expression

Nucleus-encoded factors control the expression of the plastid genome. Most genetic studies addressing the role of nuclear genes in chloroplast gene expression have been carried out with either *Zea mays* (maize), *Arabidopsis thaliana* or *Chlamydomonas reinhardtii* (Barkan et al., 1994; Meurer et al., 1996a; Rochaix et al, 2004). The majority of the factors identified by genetic approaches are specifically required for the expression of small subsets of chloroplast genes and are involved in post-transcriptional steps (Barkan and Goldschmidt-Clermont, 2000). They may also serve to couple chloroplast gene expression with the assembly of the protein products into the large complexes of the photosynthetic apparatus.

Nuclear encoded factors function in each step in plastid gene expression, including RNA splicing, processing and stability, and translation. The maize genes *crs1* and *crs2* are required for the splicing of chloroplast group II introns (Jenkins et al., 1997). Mutations in *crs1* lead to a specific defect in the splicing of the *atpF* intron, whereas mutations in *crs2* disrupt the splicing of several group II introns (Jenkins et al., 1997; Vogel et al., 1999).

A nuclear gene in *Chlamydomonas reinhardtii* was identified, that is likely to be a component of the general 3´end processing machinery; mutations in this gene – called *crp3* – have been described (Levy et al., 1997 and 1999).

Arabidopsis hcf109 mutants accumulate reduced levels of transcripts from four polycistronic transcription units (*psbB*, *psbD*, *ndhC*, *ndhH*) (Meurer et al., 1996b). *Run-on* transcription analysis demonstrated that this is due to a defect in RNA stability rather than in transcription (Meurer et al., 2002).

In vascular plants, only two nuclear genes have been found where a mutation disrupts the translation of subsets of chloroplast mRNAs, contrasting with the frequent recovery of this type of mutant in *Chlamydomonas* (Barkan and Goldschmidt-Clermont, 2000). The maize gene *atp1* is required specifically for the translation of the chloroplast atpB/E mRNA (McCormac et al., 1999) whereras mutations in the maize gene *crp1* disrupt the translation of a subset of plastid mRNAs, namely *petA* and *petD* (Barkan et al., 1994). All these examples for nucleus mutations affecting chloroplast gene expression not only disrupt the expression of individual genes but are also involved in post-transcriptional steps.

7. *Arabidopsis* as a model organism

Over the last years, *Arabidopsis thaliana*, a member of the mustard family (*Brassicaceae*), has become a model organism for plant cellular and molecular biological studies due to its small sized genome, the short life cycle, well established transformation techniques and the large number of offspring. After the complete sequencing of the relatively small *Arabidopsis* genome (five chromosomes, 125 Mb, Arabidopsis Genome Initiative, 2000) and the annotation of its genome, assigning a function to an isolated gene has become a new challenge. The classical "forward" (phenotype-related) genetic approach is the method of choice for the identification of mutants isolated by phenotype screening.

The genome of *Arabidopsis thaliana* contains around 25,500 genes (The Arabidopsis Genome Initative, 2000). Approximately 50% of these genes are known by their function either because they share sequence homologies with genes of known function or as a result of experimental efforts. The protein sequence of the remaining 50% of genes could be searched by prediction programs such as ChloroP (Emanuelsson et al., 1999) to obtain information about intracellular localisation. As only 87 proteins are encoded in the plastid DNA of *Arabidopsis*, all the other polypeptides of the chloroplast are encoded in the nucleus and posttranslationally imported into the organelle. In a proteome-wide search between 1,900 and 2,500 proteins containing a chloroplast target sequence were predicted (Abdallah et al., 2000; Martin, 2003). Of these proteins, around 30% are derived from cyanobacterial ancestors indicating a conserved function for these proteins.

8. Functional genomics

The screening of mutant populations with altered photosynthetic performance has been successfully performed to elucidate mechanisms controlling photosynthesis. Two widely used indicators of defects associated with photosynthesis are alterations in pigmentation and chlorophyll fluorescence. In general, every mutation that affects the photosynthetic electron transport chain can be detected as an increase in the fraction of absorbed energy re-emitted as fluorescence. This approach was used for the identification of *hcf* (high chlorophyll fluorescence) mutants of cyanobacteria, *Chlamydomonas rheinhardtii* and *maize*. Due to the relatively low sensitivity of this method severe effects of the photosynthetic electron transport cause seedling lethality under photoautotrophic conditions and complicate the analysis of the *hcf*-mutants. So far, several *hcf*-mutant collections have been described (Barkan et al., 1994; Meurer et al., 1996a; Rochaix et al, 2004) – from *Arabidopsis thaliana* 34 *hcf*-mutants have been identified and described (Meurer et al., 1996a). The majority of these *hcf*-mutants is lethal at the seedling stage and displays a decrease in photosynthetic electron transport activity.

9. Function of PsaJ in higher plants

In plants, the two low molecular mass subunits, PsaF and PsaN, have been implicated in the interaction between PSI and plastocyanin (Haldrup et al., 2000). PSI-N is unique to higher plants and is entirely located in the thylakoid lumen. However, the recently published structural model of higher plant PSI based on a crystal structure at 4.4 Å does not reveal the presence of PSI-N (Ben-Shem et al., 2003) and cross-linking experiments have shown little interaction between PsaN and other small PSI subunits although putative cross-linking products with PsaG and PsaF were found (Jansson et al., 1996).

PsaF contains one transmembrane helix and is exposed both to the lumen and to the stroma: its N-terminal domain is situated in the lumen (Ben-Shem et al., 2003) whereas the C-terminus is in contact with PsaE on the stromal side (Fromme et al., 2001). PsaF and luminal interhelical loops of PSI-A and PSI-B form a docking site for PC or Cyt c_6 (Farah et al., 1995; Hippler et al., 1997, 1998, 2002; Sommer et al., 2002). In plants, which only use PC as an electron donor to PSI, an extended aminoterminal domain contributes to a helix-loop-helix

motif (Ben-Shem et al., 2003) that specifically enables more efficient plastocyanin binding and, as a result, two orders of magnitude faster electron transfer from PC to P700 (Hippler et al., 1996).

Based on biochemical and structural studies predominantly in cyanobacteria it has been suggested that the small, membrane integral subunits such as PsaF, -I, -J, -K and –L mainly function in the stabilization of the antenna system and the quaternary structure of photosystem I (Fromme et al., 2001). PsaJ is a hydrophobic low molecular mass subunit with one transmembrane helix that is located close to PsaF (Jordan et al., 2001; Ben-Shem et al., 2003). The N-terminus of PsaJ is located in the stroma, the C-terminus in the lumen (Fromme et al., 2001). In cyanobacteria, PSI-J binds three chlorophylls and is in hydrophobic contact with carotenoids (Jordan et al., 2001), whereas in plants only two chlorophyll molecules are bound, which are probably important for the energy transfer between LHCI and the PSI core (Ben-Shem et al., 2003).

In cyanobacteria, PsaJ interacts with PsaF (Xu et al., 1994a). A *psaJ* knock out in *Synechocystis* PCC 6803 contained only 20% PsaF subunit compared to wild-type (Xu et al., 1994b). The corresponding *psaJ* knock out in *Chlamydomonas* contained wild-type levels of PSI-F and PSI, and the cells were able to grow photoautotrophically. A large fraction of the mutant PSI complexes displayed slow kinetics of electron donation from PC or Cyt c_6 to P700: The absence of PsaJ did not alter the half-lives of the different kinetic phases, but lead to the formation of two subpopulations of PSI complexes which differed with respect to electron transfer to P700$^+$. One population behaved like wild-type with fully functional PsaF and the other had characteristics similar to a PsaF deficient strain (Fischer et al., 1999). It was concluded that in 70% of the PSI complexes lacking PsaJ, the N-terminal domain of PsaF is unable to provide a binding site for either PC or Cyt c_6 that in turn lead to electron transfer to P700$^+$ and was explained by a displacement of this domain. Thus, PsaJ does not appear to participate directly in binding of PC or Cyt c_6 but plays a role in maintaining a precise recognition site of the N-terminal domain of PsaF required for fast electron transfer from PC and Cyt c_6 to PSI (Fischer et al., 1999).

II. Materials and Methods

1. Materials

1.1 Working materials

Chemicals used in this work were of p.a. quality and were purchased from the following companies, if not otherwise mentioned: Applichem (Darmstadt, Germany), Biozym (Oldendorf, Germany), Fluka (Steinhein, Germany), ICN Biomedicals GmbH (Eschwege, Germany), Merck (Darmstadt, Germany), Pharmacia (Uppsala, Sweden), Roth (Karlsruhe, Germany), Serva (Heidelberg, Germany), Sigma-Aldrich Chemie GmbH (Taufkirchen, Germany), and USB (Cleveland, USA). Enzymes were obtained from Clontech (Palo Alto, USA), Invitrogen (Karlsruhe, Germany), MBI Fermentas (St. Leon-Rot, Germany), New England Biolabs (Frankfurt/Main, Germany), Promega (Mannheim, Germany), Qiagen (Hilden; Germany), Roche Diagnostics (Mannheim, Germany), and Stratagene (Heidelberg, Germany). Radioactive nucleotides and [^{35}S]-methionine were purchased from Amersham Biosciences Europe GmbH (Freiburg, Germany). Other materials were obtained from Biomol (Hamburg, Germany), Eppendorf (Hamburg, Germany), Greiner Bio-One GmbH (Frickenhausen, Germany), Millipore (Eschborn, Germany), Pall Bio Support Division (Dreieich, Germany), Qiagen (Hilden, Germany), and Schleicher and Schüll (Dassel, Germany). The manufacturers of commercial devices are mentioned in the text.

1.2 Plant material

The *apo1* mutation, accession Wassilewskija, was selected from a T-DNA-insertion collection (Feldmann 1991) obtained from the Arabidopsis Biological Resource Centre (Ohio State University, Columbus, USA).

1.3 Bacterial strains and vectors

E. coli DH5α   (Bethesda Res. Lab., 1986)

Agrobacterium tumefaciens GV3101 (pMP90RK)   (Meurer *et al.*, 1998a)

The vector pBluescript KSII+ (Stratagene, Heidelberg) was used for standard cloning. The plant binary expression vector pSEX001-VS (Reiss *et al*., 1996) was used for cloning of cDNAs under the control of the 35S RNA promoter of *Cauliflower mosaic virus* in complementation studies (Figure 1).
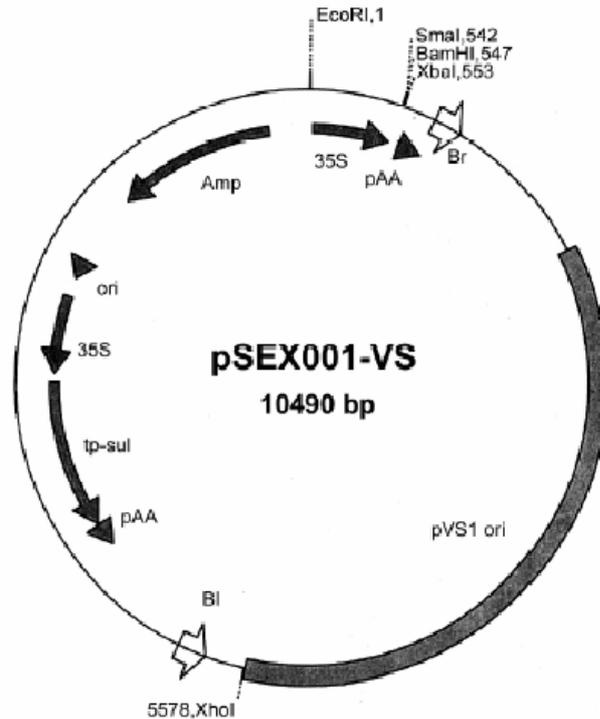
Figure 3: Map of the plant binary expression vector pSEX001-VS. EcoRI,1 – EcoRI site at nucleotide position 1; SmaI,542 – SmaI site at nucleotide position 542; BamHI,547 – BamHI site at nucleotide position 547; XbaI,552 – XbaI site at nucleotide position 552; 5578,XhoI – XhoI site at nucleotide position 5578; Br and Bl – *Agrobacterium* T-DNA right and left border sequences, respectively; 35S – CaMV 35S RNA promoter; pAA – polyadenylation signal from CaMV; ori – *E. coli* origin of replication; tp-sul – sulfonamide-resistance gene equipped with a chloroplast targeting peptide; Amp – ampicillin-resistance gene; pVS1 – *Agrobacterium* origin of replication.

1.4 Hybridisation probes for Northern analysis

Hybridization probes are listed below. Additional plastid DNA probes were generated by amplifying specific regions of the *Arabidopsis* plastid chromosome using oligonucleotide primers synthesized by MWG-Biotech (Ebersberg, Germany).

Table 1: Hybridisation probes used for Northern analysis.

Gene	Plasmid	Fragment	Reference
PsaA	W3	BamHI/KpnI	Westhoff *et al.*, 1991
PsaC	pR668HSI	HincII/SspI	Kubicki *et al.*, 1996

PsbA	pSoP2520.3	PstI/XbaI	Westhoff *et al.*, 1991
RbcL	pSoP2458	PstI/BamHI	M. Streubel and P. Westhoff

Gene	Amplified Gene	Primer designation	Primer sequence (5′→3′)
Cab	cab-f. cab-r.		5′-CTC ACC GCA ATG GCC GCC TCG ACA ATG GC-3′ 5′-GAC GAA GTT GGT AGC GAA GGC CCA TGC-3′
PsaI	psaI-f psaI-r		5′-CCG CGC GTA ATA CGA CTC ACT ATA GGA GTA AAT CGA GGT ACC CCT-3′ 5′-AGC GGA TCT AAA CAA TC-3′
PsaJ	psaJ-f psaJ-f		5′-TCG GTA AGA AAG AAG GGG ATG-3′ 5′-CAG TTA ATT CGA ACT TGA GC-3′

1.5 Oligonucleotides

Table 2: Oligonucleotide primers used for amplification of genes and quantification of mRNAs

Experiment	Amplified gene	Primer designation	Primer sequence (5′→3′)
Real-time RT-PCR *(apo 1)*		F13011-50.305f.	5′-GCT TCT GGT TTC TCC TGC TTG TAG AGG TG-3′
		F13011-50.575r.	5′-ACT TGT CTG CTC TCT ATG CTT CTG ATT-3′
		internal control, with 18S rDNA primers	5′-GCT CAA AGC AAG CCT ACG CTC TGG-3′
			5′-GGA CGG TAT CTG ATC GTC TTC GAG CC-3′
Complementation (*apo1*)	*apo 1* genomic DNA	apo1-f. (Komp.1)	5′-CAC GGT CTG AGC TGA TTG CGT GTT CTC-3′
		apo1-r. (Komp.2)	5′-CCA AGG ACT TAT GCG ACC ATG TCG GCT TCC-3′
PE	psaA	psaA-PE 5′IRD 700	5′-GTG AGC ATC AGC ATG TAG GTT CCA GAT CC-3′
iPCR		Sal1 (LB Sal1)	5′-CAC CTG TCC TAC GAG TTG C-3′
		Out2 (LB Out2)	5′-GCA TAG ATG CAC TCG AAA TCA GCC-3′
GFP	APO1 cDNA	apoGFP-f.	5′-ACT TAT ATA GTC GAC ATG CTT CTG GTT TCT-3′
		apoGFP-r.	5′-GAT ATC CAC GTC GAC CGA TCA CTC TCT TCC-3′
RACE		apo1-r2	5′-ACT TGT CTG CTC TCT ATG CTT CTG ATT-3′

Import	APO1 cDNA	apoT7 F13011-51680r.	5´-GTA ATA CGA CTC ACT ATA GGG CTT ATA TAG TCA ACA-3´ 5´-CCA AGG ACT TAT GCG ACC ATG TCG GCT TCC-3´
Mapping		nga128 Chr1-110	5´-CAC ACA TAT TAA CGA GTG GAT TGA CG-3´ 5´-GGA CTC AAA TAT GTG ACA AGA GTA AGA CTC-3´

1.6 cDNA library

A Uni-ZAP^{TM}XR cDNA library (Stratagene, La Jolla, USA) was prepared from RNA of *Arabidopsis* leaves, ecotype Columbia, according to the manufacturer′s instructions and was kindly provided by Dr. Csaba Koncz (Max-Planck-Institut für Züchtungsforschung, Köln, Germany).

1.7 Media, solutions and buffers

TE buffer:
10 mM Tris-HCl, pH 8.0
1 mM Na$_2$EDTA

10x TBE buffer:
108 g/l Tris, pH 8.2 - 8.4
55 g/l M boric acid
7.4 g/l Na$_2$EDTA

MOPS buffer:
20 mM MOPS
5 mM Na-acetate
1 mM Na$_2$EDTA, pH 7.0

Materials

20x SSC buffer:

3 M NaCl

0.33 M Na-citrate, pH 7.0

MS-medium:

1x MS-salts (Murashige and Skoog, 1962)

1.5% sucrose

2.5 mM MES-NaOH, pH 5.7

0.3% gelrite

Infiltration medium:

5% sucrose

0.05% Silvet L-77 (Clough and Bent, 1998)

YEB medium:

5 g/l beef extract

5 g/l bacteriological peptone

5 g/l sucrose

2 ml 1 M $MgCl_2$

supplemented with 20 g/l agar for solid medium

LB-medium:

10 g/l peptone (bacteriological grade)

5 g/l yeast extract

10 g/l NaCl, pH 7.2

supplemented with 15 g/l agar for solid medium

Hybridisation buffer:

250 mM Na_2HPO_4, pH 7.2

7% (w/v) SDS

2.5 mM EDTA (Church and Gilbert, 1984)

Washing solution 1:

2.5x SSC

1% SDS

Washing solution 2:

1x SSC

1% SDS

Washing solution 3:

0.5x SSC

1% SDS

Materials

Washing solution 4:

0.2x SSC

1% SDS

Washing solution 5:

0.1x SSC

0.5% SDS

Solutions and buffers which are not mentioned otherwise were prepared as described in Sambrook *et al*., (1989).

1.8 Antibodies

Table 3: Antibodies used for Western analysis

Protein or protein complex	Subunit	Source of an antibody
Photosystem I	PsaA/B	R. Nechushtai (Hebrew University, Jerusalem, Israel)
	PsaC	R. Herrmann
	PsaD	R. Herrmann
	PsaF	R. Herrmann

LHCI	Lhca1	Agri Sera AB (Vännäs, Sweden)
	Lhca2	Agri Sera AB (Vännäs, Sweden)
	Lhca3	Agri Sera AB (Vännäs, Sweden)

	Lhca4	Agri Sera AB (Vännäs, Sweden)
Photosystem II	PsbB	R. Berzborn (Ruhr-University Bochum, Bochum, Germany)
	PsbC (CP43)	J. Mullet (Texas A&M University, College Station, Texas, USA)
	PsbD (D2)	J. Mullet
	PsbO (PSII-O)	R. Berzborn

LHCII	Lhcb1	Agri Sera AB (Vännäs, Sweden)
	Lhcb2	Agri Sera AB (Vännäs, Sweden)
Cytochrome b_6f complex	PetA	R. Herrmann
	PetB	R. Berzborn
	PetE	n.d.
	PetH	n.d.
ATP synthase	α subunit (CF$_1$ α, AtpA)	R. Berzborn
	Subunit II (CF$_o$ II, AtpG)	R. Berzborn
Ferredoxin		R. Scheibe (Universität Osnabrück, Osnabrück, Germany)

Ferredoxin-thioredoxin reductase	FtrA	P. Schürmann (Université de Neuchâtel, Neuchâtel, Switzerland)
	FtrB	P. Schürmann
Ndh-complex	NdhA	Steinmüller
	NdhH	Steinmüller

n.d.: source not known

2. Methods

2.1 Cultivation of bacteria

The *E.coli* strain was propagated in LB medium or on LB-agar plates at 37°C as described in Sambrook *et al*., 1989. For transformation with plasmids carrying ampicillin resistance, 70 μg/ml ampicillin were added to the medium. The *Agrobacterium* strain was grown at 28°C in YEB medium supplemented with 100 μg/ml rifampicin and 25 μg/ml kanamycin. For transformation with binary vector carrying ampicillin resistance, 100 μg/ml carbenicillin were used.

2.2 Seed sterilization, medium and culture conditions

Wild-type and mutant plants were grown under green house conditions or on sucrose-supplemented medium as described in Meurer *et al*. (1996a). In all analyses phenotypically wild-type plants of heterozygous progenies grown under the same conditions were compared to *apo1*. Selection of mutant plants was facilitated by a chlorophyll fluorescence video imaging system (FluorCam690M, Photon Systems Instruments, Brno, Czech Republic). The *hcf* mutants were readily distinguishable from wild-type plants because of their failure to quench chlorophyll fluorescence. Propagation of the lethal *hcf* mutants occurred via heterozygous offsprings grown on soil. In all experiments three-week-old plants were used if not differently indicated.

2.3 General molecular biological methods

Phenol/chloroform extraction, precipitation, gel electrophoresis, staining and quantification of nucleic acids were performed according to standard protocols (Sambrook et al., 1989). DNA fragments were purified from agarose gels using the QIAEX®-II Gel extraction kit and PCR products were purified with the QIAquick® PCR purification Kit (Qiagen, Hilden). Restriction and ligation of DNA fragments were performed according to the manufacturers instructions.

Plasmid DNA for sequencing or cloning was isolated using QIAprep Spin Miniprep Kit (Qiagen, Hilden, Germany). The alkaline lysis protocol (Birnboim and Doly, 1979) was used to obtain plasmid DNA after ligation. Preparation of competent cells and heat-shock transformation of *E. coli* occurred according to Hanahan (1983).

2.4 Vector construction, chloroplast transformation and plant material

The region of the tobacco chloroplast genome containing 700bp upstream and downstream of the *psaJ* reading frame was amplified using PCR. The 1535bp fragment was ligated into the SacI and BamHI sites of pUC19. The *psaJ* knock-out allele was generated by digestion of this construct with ScaI and a chimeric *aadA* gene conferring resistance to aminoglycoside antibiotics (Svab and Maliga, 1993) was inserted into this ScaI site to disrupt *psaJ* and to facilitate selection of chloroplast transformants. ScaI causes a disruption of the 132bp *psaJ* coding region after nucleotide 38. A plasmid clone carrying the *aadA* gene in the same orientation as *psaJ* yielded the transformation vector pPsaJ (Fig. 12).

Chloroplasts of *Nicotiana tabaccum* cv. Petit Havanna were transformed by particle bombardment of leaves (Svab and Maliga, 1993). Selection and culture of transformed material as well as assessment of plastome segregation and of the homoplastomic state were performed essentially as described in Swiatek et al. (2003). The material was maintained on agar-solidified MS-medium (Murashige and Skoog 1962) containing 2% sucrose, and grown in 12 h dark/light cycles at $25^{O}C$ and 20 µmoles photons m^{-2} s^{-1}, under selective conditions with 500 µl/ml spectinomycin. For thylakoid isolation and physiological measurements, wild type and transformed plants were planted in compost and kept under growth chamber conditions in 8h light and 120 - 140 µmol photons m^{-2} s^{-1}.

2.5 DNA analysis

2.5.1 Polymerase chain reaction (PCR)

For PCR amplifications of DNA templates 0.5 mM oligonucleotide primers, 0.2 mM dNTPs, 5 mM $MgCl_2$ and 2.5 U Taq polymerase were used in a 20 µl final reaction volume. An initial

denaturation step was performed at 95°C for 3 min, and afterwards 32 cycles of denaturation (95°C for 15 sec), annealing (58 - 62°C for 15 sec) and extension (72°C for 1 min per 1 kb DNA) were performed followed by a final extension step at 72°C for 8 min.

2.5.2 DNA isolation

DNA was isolated from young *Arabidopsis* leaves (approx. 0.5 cm^2). Plant material was homogenised in 1.5 ml-Eppendorf tubes using a mechanical stirrer RW16 basic (Kika Labortechnik, Staufen, Germany) for approx. 5 sec, and immediately afterwards 400 µl extraction buffer (0.2 M Tris/HCl, pH 7.5; 0.25 M NaCl; 0.025 M EDTA and 0.5% (w/v) SDS) was added. After a short vortexing step, the extract was centrifuged for 3 min at 16,000 g at room temperature. 300 µl supernatant were transferred to a new Eppendorf tube and 300 µl isopropanol was added. The mixture was vortexed, incubated at room temperature for 2 min and centrifuged for 5 min at 16,000 g at room temperature or at 4°C. The supernatant was discarded, and the pellet was air-dried and resuspended in 50 µl TE buffer. For PCR amplification 2 µl DNA were used.

2.5.3 iPCR

T-DNA flanking sequences were isolated by inverse PCR. SalI-digested genomic DNA was religated and subsequently subjected to PCR using the primers 5´-CAC CTG TCC TAC GAG TTG C-3´ and 5´-GCA TAG ATG CAC TCG AAA TCA GCC-3´. PCR products were cloned and sequenced.

2.5.4 GFP fusion

PCR products of the APO1 cDNA were generated using primers 5´-ACT TAT ATA GTC GAC ATG CTT CTG GTT TCT-3´ and 5´-GAT ATC CAC GTC GAC CGA TCA CTC TCT TCC-3´ and cloned into the SalI site of the GFP expression vector pOL-LT (Mollier et al., 2002), producing a translational fusion of the APO1 protein containing APO motif 1 with GFP.

GFP was transiently expressed in tobacco (*Nicotiana tabacum*) protoplasts using the polyethylene glycol protocol (Lyznik et al., 1991). Fluorescence was visualized using a fluorescence microscope equipped with a digital camera (Axioplan; Zeiss, Jena, Germany).

2.5.5 Radioactive labelling of DNA

DNA labelling was performed using the Random Primed DNA Labeling Kit (Roche Molecular Biochemicals, Mannheim, Germany) according to the method of Feinberg and Vogelstein (1983).

2.5.6 Hybridisation of nucleic acids

All hybridisations were performed overnight in hybridisation buffer (see Chapter 2.1.7) at 62°C (Church and Gilbert, 1984). Prehybridisations were carried out in the same buffer for at least two hours. After hybridisation, filters were washed for 30 min in each of the washing solutions 1 to 5 (see Chapter 2.1.7). For exposure filters were sealed in plastic foils and analysed by phosphorimaging (BASIII Fuji Bio Imaging plates and BAS2000 software package and the AIDA software package v3.25 beta; Raytest, Straubenhardt, Germany).

2.6 RNA analysis

2.6.1 Isolation of total RNA of *Arabidopsis*

Nucleic acids were isolated from 1 - 2 g of leaf material in 8 ml homogenisation solution (0.33 M sorbitol; 0.2 Tris - NaOH, pH 9.0; 0.3 M NaCl; 10 mM EDTA; 10 mM EGTA; 2% SDS) mixed with 4 ml phenol and 4 ml chloroform at 40°C. Total RNA was selectively precipitated with 2 M LiCl (Lizardi 1983; Westhoff *et al*., 1993). PolyA+ mRNA was isolated using OligodT-beads according to the manufacturer´s instructions (Dynal, Oslo, Norway) and used for RACE experiments.

2.6.2 Northern analysis

For Northern analysis 8 μg of total cellular RNA was used. RNA was denatured through incubation with 30% glyoxal (McMaster and Carmichael, 1977), electrophoretically separated in 1.2% agarose gels in MOPS buffer and transferred onto a Biodyne A nylon membrane (0.2 μm; Pall, Dreieich, Germany) in 20x SSC buffer (Grüne and Westhoff, 1988). RNA was fixed to the membrane by UV radiation. EcoRI/HindIII-digested and glyoxylized lambda DNA was used as a molecular weight standard.

2.6.3 RNA gel blot analysis of tobacco

Nucleic acids were isolated from 1 – 2 g leaf material in 8 ml homogenisation solution (0.33 M sorbitol; 0.2 M Tris-HCl, pH 9.0; 10mM EDTA; 10mM EGTA; 2% SDS) mixed with 4 ml phenol and 4 ml chloroform at 40ºC. Total RNA was selectively precipitated with 2 M LiCl (Lizardi 1983). For Northern analysis 8 μg of total cellular RNA was used. RNA was denatured through incubation with 30% glyoxal (McMaster and Carmichael, 1977), electrophoretically separated in 1.2% agarose gels in MOPS buffer and capillary transferred onto a Biodyne A nylon membrane (0.2 μm; Pall, Dreieich, Germany) in 20x SSC buffer (Grüne and Westhoff, 1988). RNA was fixed to the membrane by UV radiation. DNA labelling was performed using the Random Primed DNA Labeling Kit (Roche Molecular Biochemicals, Mannheim, Germany) according to the method of Feinberg and Vogelstein (1983).

2.6.4 Primer extension

Primer extension reactions were performed with 50 mg of DNase-treated RNA using the Superscript II reverse transcriptase (Invitrogen, Karlsruhe, Germany) and the fluorochrome-labeled primer 5´- GTG AGC ATC AGC ATG TAG GTT CCA GAT CC - 3´ annealing to the *psaA* 5´ coding region. Sequencing and product analysis was performed using the LI-COR 4200IR2 two-laser system (MWG Biotech, Ebersberg, Germany).

2.6.5 Reverse transcription (RT)-PCR

Reverse transcription was performed with 1 µg total RNA using SuperScript II RNase H⁻ Reverse Transcriptase (Invitrogen, Karlsruhe, Germany) and either hexanucleotides (Roche Molecular Biochemicals, Mannheim, Germany) or gene-specific primers according to the manufacturers instructions. DNase I (RNase-free; Roche Molecular Biochemicals, Mannheim, Germany) was used for removal of DNA from RNA preparations prior to RT-PCR reactions. In case that some contaminating DNA remained in the RNA sample, primers were designed that anneal to sequences in exons at both sides of an intron to differentiate between amplification of cDNA and amplification of residual, if any, DNA. With this approach PCR products derived from genomic DNA are longer compared to those derived from the intronless mRNA. The 5´ end of the APO1 cDNA was determined by RACE experiments with the 5´ RACE primer SMART (BD BiosciencesClontech, Palo Alto, CA) and the gene-specific primer apo1-r2 (5´-ACT TGT CTG CTC TCT ATG CTT CTG ATT-3´) located within the coding region.

2.6.6 Quantitative real-time RT-PCR

Quantitative two-step RT-PCR for *apo1* and wild-type mRNA was performed using the LightCycler system (Roche Molecular Biochemicals, Mannheim, Germany) applying the SYBR Green protocol (Wittwer et al., 1997). Real-time PCR was performed with APO1 exon-specific primers (5´-GCT TCT GGT TTC TCC TGC TTG TAG AGG TG-3´ and 5´-ACT TGT CTG CTC TCT ATG CTT CTG ATT-3´) and, as an internal control, with 18S rDNA primers (5´-GCT CAA AGC AAG CCT ACG CTC TGG-3´ and 5´-GGA CGG TAT CTG ATC GTC TTC GAG CC-3´). Serially diluted samples of the APO1 cDNA were used for the calibration curve.

2.6.7 Polysome analysis

Isolation of polysomes from leaves of 3-week-old plants was performed essentially as described in Barkan (1998). Polysome aliquots were layered onto 15% to 55% sucrose gradients and centrifuged for 65 min at 272.000 g and 48°C in a SW60 Ti rotor (Beckman, Munich, Germany).

Fractions of 0.4 ml were collected, and the RNA obtained was subjected to RNA gel blot analysis.

2.7 Translation inhibition experiment

For translation inhibition, three-week-old wild-type and *apo1*-plants were used. Hypocotyls were clipped in a ½ MS solution containing 400 mg/l lincomycin to avoid air embolism. Control plants were incubated for the same time in a solution containing ½ MS nutrients. Total RNA was isolated from the harvested material and used for Northern analysis. The *psaA* and *psbA* probes used for the hybridisations are listed in Table 1.

2.8 Protein and pigment analysis

2.8.1 Measurement of protein and chlorophyll concentration in *Arabidopsis*

Protein concentrations were measured according to Bradford (1976). Protein amounts of mutants were equalised to amounts in wild-type (10 µg) according to silver-stained gels (Blum *et al*., 1987). Chlorophyll concentrations were measured according to Arnon (1949).

2.8.2 Sodium dodecyl sulfate polyacrylamide gel electrophoresis (SDS-PAGE).

Soluble and membrane proteins of three-week-old plants were isolated and separated by SDS-PAGE as described in Meurer *et al*., (1996b).

2.8.3 Immunological analysis

Membrane proteins of 3-week-old plants were isolated substantially as described (Meurer et al., 1996a). The supernatant of the first centrifugation, which contained the soluble proteins, was precipitated with 15% trichloroacetic acid. The sediment was washed twice with 80% acetone and resuspended in 100 mM Na_2CO_3, 10% sucrose, and 50 mM dithioerythritol. Proteins separated by SDS-PAGE were transferred to polyvinylidene difluoride membranes (Amersham Buchler, Braunschweig, Germany), incubated with specific antibodies (Meurer et

al., 1996a), and visualized by the enhanced chemiluminescence technique (Amersham Buchler).

2.8.4 Radioactive labeling of plastid membrane proteins

In vivo labeling of leaf proteins was performed as described (Meurer et al.,1996b), with the exception that the hypocotyls of plants were first cut in the antibiotic-containing solution and subsequently immersed into the appropriate medium supplemented with [35S]Met (50 mCi; specific activity >1000 Ci/mmol) for 20 min.

2.8.5 Separation of thylakoid membrane complexes

Approximately 1 g *Arabidopsis* seedlings were homogenized in 0.3 M sorbitol, 5 mM $MgCl_2$, 20 mM Tricine/KOH (pH 8.4), 20 mM EDTA, 0.1% (w/v) BSA. The homogenate was filtered through two Miracloth layeres (100 μm, Calbiochem, La Jolla, USA) and centrifuged for 3 min at 2,370 rpm in a table centrifuge at 4°C. The pellet containing the membrane fraction was resuspended in 1 ml TMK buffer (10 mM Tris-HCl, pH 6.8, 10 mM $MgCl_2$ and 20 mM KCl). The suspension obtained was incubated for 10 min on ice and then centrifuged (3 min at 650 g). The pellet was washed twice with 500 μl TMK buffer to remove soluble proteins. Membrane fractions equivalent to 40 – 120 μg chlorophyll were resuspended in 40 μl TMK buffer, and 120 μl of 2% (w/v) β-dodecylmaltoside in TMK was added to obtain a final concentration of 1.5% (w/v). The suspension was incubated for 10 min on ice to solubilize the major thylakoid membrane protein complexes and centrifuged (10 min, 21,000 g in a table centrifuge at 4°C). The supernatant containing the thylakoid lysate was loaded onto a linear 0.1 – 1.0 M sucrose gradient and centrifuged for 17 h at 125,000 g at 4°C in a SW60Ti rotor (Beckman, Munich, Germany). Fractions of 0.2 ml where collected from bottom-to-top and used for SDS-PAGE and Western analysis.

2.8.6 Protein import into chloroplasts

The APO1 cDNA was amplified with primers 5´ - GTA ATA CGA CTC ACT ATA GGG CTT ATA TAG TCA ACA - 3´ and 5´ - CCA AGG ACT TAT GCG ACC ATG TCG GCT TCC - 3´ that generate a T7-promoter upstream of the coding region, allowing *in vitro* trans-

cription. Isolated chloroplasts were incubated for 0, 5, 10, and 20 min with labeled *in vitro* translation products of *apo1* generated in cell-free wheat germ extracts in the presence of [35S]Met (Roche Molecular Biochemicals). Chloroplasts were purified, washed twice, treated with thermolysin when indicated, and the isolated proteins were subjected to SDS-PAGE (Lezhneva et al., 2004). Gels were dried and exposed to phosphor imaging plates (BASIII Fuji Bio Imaging plates and BAS2000 software package (Tokyo, Japan) and the AIDA software package version 3.25 beta; Raytest, Straubenhardt, Germany).

2.8.7 Isolation of thylakoid membranes and PSI assemblies from tobacco

Leaves from 6- to 8-week-old plants were used for isolation of thylakoids as described previously (Haldrup et al., 1999). PSI particles were isolated from thylakoids after solubilization with dodecyl-β-D-maltoside and sucrose density ultracentrifugation as described in Jensen et al. (2000). Chl content and the Chl a/b ratio were determined in 80% acetone according to Lichtenthaler (1987). The samples were frozen in liquid nitrogen and stored at -80ºC.

2.8.8 Chlorophyll content per leaf area

Total leaf chlorophylls were extracted by boiling leaf disks in 95% EtOH for 30 min. After cooling to room temperature and volume adjustment the Chl content and Chl a/b ratio was determined in 95% EtOH according to Lichtenthaler (1987).

2.8.9 Immunoblotting

Immunoblotting analysis was performed essentially as described previously (Jensen et al., 2000) using antibodies directed against subunits of the various thylakoid membrane complexes as indicated in the figure legends. Primary antibodies were detected using a chemiluminescent detection system (Immun-Star, Bio-Rad and Super-Signal, Pierce) according to the instructions of the manufacturer. The chemiluminescent signal produced was recorded digitally using a cooled CCD camera with the AC1 AutoChemi System (Ultra-Violet Products Ltd, Cambridge, UK).

The exposure time was set to 5 minutes, with accumulative snapshots at 30 second intervals. Signal intensity was quantified using the LabWorks Analysis Software (Ultra-Violet Products Ltd, Cambridge, UK).

2.9 Spectroscopic and fluorimetric methods

2.9.1 Chlorophyll *a* fluorescence analysis in *Arabidopsis*

Chlorophyll *a* fluorescence analyses were performed using plants of the same age grown under identical conditions. A pulse amplitude–modulated fluorometer (PAM101; Walz, Effeltrich, Germany) equipped with a data acquisition system (PDA-100; Walz) and a personal computer using Wincontrol version 1.72 software (Walz, Effeltrich, Germany) for data collection were used to measure and analyze *in vivo* chlorophyll *a* fluorescence. The following settings were used for the PAM101 unit: light intensity, 4; gain, 6; damping, 9. After induction, saturating pulses of 4,000 $\mu E \, m^{-2} \, s^{-1}$ light intensity and 1 s duration were applied in 30 s intervals to estimate quenching parameters (Meurer *et al*., 1996b).

2.9.2 Light-induced change of the P700 redox state

Light-induced changes of the P700 redox state were recorded by absorbance changes at 830 nm, with the above described PAM system equipped with a dual wavelength emitter-detector unit (Meurer *et al*., 1996b). Multiple turn-over flashes of 50 μs were induced by a Xenon lamp (Walz, Effeltrich, Germany) and saturating light pulses of 1 s were applied by halogene lamps.

2.9.3 Photochemical and non-photochemical chlorophyll *a* fluorescence quenching

Photochemical (qP) and non-photochemical (NPQ) chlorophyll *a* fluorescence quenching at room temperature were performed using the PAM system described in Chapter 2.2.9.1. The actinic light intensity was 20 $\mu E \, m^{-2} \, s^{-1}$, and the intensity of the saturating light pulses (1 s, 20 s intervals) used for detection of the quenching parameters during induction was 4000 $\mu E \, m^{-2} \, s^{-1}$.

2.9.4 Low temperature chlorophyll fluorescence spectra

Chlorophyll fluorescence emission spectra at 77 K were recorded with a Hitachi fluorometer (model F-3010; Hitachi, Tokyo, Japan), as described in Meurer *et al.* (1996a). Spectra were normalized with respect to equivalent long-wavelength emission bands.

2.9.5 Fluorescence measurements in tobacco

Fluorescence emission spectra at 77 K were recorded on intact leaves from dark-adapted plants or PSI particles using a bifurcated light guide connected to a spectrofluorometer (Photon Technology International, Lawrenceville, NJ). The excitation light had a wavelength of 435 nm, and emission was detected from 650 to 800 nm. Standard fluorescence parameters - the Q_A redox state ($1-q_P$), PSII quantum yield (Φ_{PSII}), non-photochemical quenching (NPQ) under growth light conditions were performed as described in Lunde *et al.* (2003), and the parameters were calculated using the following equations, $1-q_P = (F_s-F_0')/(F_m'-F_0')$, $\Phi_{PSII} = (F_m'-F_s)/F_m'$, Φ_{PSII} (dark-adapted) $= (F_m-F_0)/F_m$ and NPQ $= (F_m-F_m')/F_m'$ for standard fluorescence.

2.9.6 NADP$^+$ photoreduction measurements and Chl/P700

The NADP$^+$ photoreduction activity of PSI was determined from the absorbance change at 340 nm as described by Naver *et al.* (1996) using thylakoids equivalent to 5 µg of Chl. Thylakoids were solubilized in 0.1% *N*-dodecyl-β-D-maltoside prior to measurements. The total P700 content was determined from the ferricyanide-oxidized minus ascorbate-reduced difference spectrum using an extinction coefficient of 64,000 M^{-1} cm^{-1} at 700 nm. The thylakoids were solubilized with 0.2% Triton X-100, and the measurements were repeated 4 - 5 times on several independent thylakoid preparations.

2.9.7 Antenna size of PSI

Functional PSI antenna size was determined from light-induced P700 absorption changes at 810 nm using the Dual Wavelenght Emitter Detector Unit ED-P700DW-E connected via PAM 101 Fluorometer (Walz, Effeltrich/Germany) to a Tektronix TDS420 oscilloscope using

thylakoids equivalent to 33 μg of chlorophyll. Thylakoids were solubilized with 0.01% digitonin prior to measurements. For each sample four traces were averaged and the measurements were repeated five times on several independent thylakoid preparations. The absorption curves were fitted with single-exponential functions, and relative antenna sizes (percent of wild-type) were calculated from the halftimes ($t_{1/2}$) with the assumption that all chlorophylls functionally connected to a reaction center contribute equally to P700 oxidation in the monitored millisecond time scale.

2.9.8 Kinetic measurements

Flash-induced P700 absorption decay was measured at 834 nm, as described previously (Naver et al., 1996; Drepper et al., 1996; Zygadlo et al., 2005) The saturating actinic pulse (532 nm, 6 ns) was produced by a Nd:YAG laser. Thylakoids (20 μg of chlorophyll) were dissolved in a final volume of 300 μl of 20 mM Tricine (pH 7.5), 40 mM NaCl, 8 mM $MgCl_2$, 0.1% digitonin, 2 mM sodium ascorbate, 6 μM 2,6-dichlorophenolindophenol and 100 μM methylviologen. The solution was incubated in darkness for 10 min on ice and centrifuged once for 10 s at 200 x g to remove starch. The sample (300 μl) was then transferred to a cuvette with a 1 cm path length and PC was added to the required concentration, from 5 - 500μM. A diode laser provided the measuring beam, which was detected using a photodiode. The signal was passed *via* a preamplifier (Tektronix ADA400A) to an oscilloscope. The time resolution with this setup is about 2.5 μs. A total of 32 absorbance transients were collected with 4 s intervals and averaged for each decay curve. The recorded absorbance changes were resolved into three exponential decay components using a Levenberg-Marquardt non-linear regression procedure. Kinetic parameters were calculated from the exponential decays essentially according to Drepper et al. (1996).

2.9.9 P700 oxidation state in WT and ΔPsaJ leaves

The redox level was monitored at 810 nm and 860 nm with a PAM 101-103 chlorophyll fluorometer (Walz, Effeltrich, Germany) connected to a dual wavelength emitter-detector unit ED 700 DW as described by Klughammer and Schreiber (Klughammer and Schreiber, 1994). The dual wavelength emitter-detector system detects strictly differential absorbance changes

(810 nm minus 860 nm) and is selective for absorbance changes caused by P700 (Klughammer and Schreiber, 1998). Oxidized P700 (ΔAmax) was recorded during far-red light illumination. The level of oxidized P700 in the leaf (ΔA) was determined during white light illumination (from 25 to 800 μmol photons m^{-2} s^{-1}). PSI acceptor side limitation was determined using 50 ms flashes from a Walz XST 103 unit. Flashes were applied during the actinic light (SF_{al}) and the far-red (SF_{fr}) illuminations and the acceptor side limitation calculated as (SF_{fr} - SF_{al})/ SF_{fr}.

2.10. Genetic methods

2.10.1 Mapping of the *apo1* mutation

For genetic crosses, male plants of the accession Landsberg erecta were used to generate the F2 mapping populations. Single mutant seedlings were chosen for mapping the APO1 gene using the microsatellite marker nga128 (http://www.arabidopsis.org/) and the marker chr1-110 (5´-CAC ACA TAT TAA CGA GTG GAT TGA CG-3´ and 5´-GGA CTC AAA TAT GTG ACA AGA GTA AGA CTC-3´) on chromosome 1 at positions 20.234 and 25.364 Mb, respectively.

2.10.2 Complementation of the *apo1* mutant

The full-length cDNA of APO1 was amplified by PCR using the 5´ end primer apo1-f (5´-CAC GGT CTG AGC TGA TTG CGT GTT CTC-3´) and the TAA stop codon–containing primer apo1-r (5´-CCA AGG ACT TAT GCG ACC ATG TCG GCT TCC-3´). The product obtained was cloned into the SmaI site of the binary plant transformation vector pS001 (Meurer et al., 1998a). Heterozygous offsprings were transformed *via Agrobacterium tumefaciens* using the floral dip method (Clough and Bent, 1998).

2.11. Sequence analysis

Nucleotide sequences were determined using the ABI377 system (Applied Biosystems, Foster City, CA). Sequences were evaluated using Sequencher 3.0 software (Gene Codes Corp., Ann Arbor, MI). Protein homologues were identified by BLAST analysis (Altschul *et al.,* 1997) of

sequenced genomes at the NCBI website (http://www.ncbi.nlm.nih.gov/Blast). Sequence alignments were performed using the programme MacMolly tetra (SoftGene GmbH; Schöneberg *et al*., 1994).

2.12 Chloroplast ultrastructure

Sample preparation for ultrastructural analysis was performed as described (Meurer et al., 1998b). Electron microscopy was performed by Prof. Dr. G. Wanner (LMU, München).

2.13 GenBank accession numbers

The GenBank accession number of *Arabidopsis* APO1 cDNA is AY466161. Accession numbers or names for other genes mentioned in this article are At5g57930.1, At5g61930.1, and At3g21740.1 (*Arabidopsis* APO2 to APO4 genes, respectively), AL662950, AK104342, AP003840, and AK064525 (rice APO1 to APO4 genes, respectively).

III. Results

Part A: Characterisation of the *apo1* mutant

1. Selection, phenotype, and growth of *apo1*

In a systematic screen for nuclear-encoded factors responsible for acclimation and maintenance of PSI biogenesis, *Arabidopsis* mutants were identified that are incapable of photoautotrophic growth (Meurer et al., 1996a). 87 mutants were selected with visible phenotypes that exhibited an albinotic, pale or *hcf* phenotype and seedling lethality. Mutant plants that were grown heterotrophically often survived, indicating photosynthetic deficiencies as primary defects. All analyses were performed with plants grown *in vitro*. On sugar-supplemented medium, the otherwise albinotic *apo1* mutant showed a very pale and high chlorophyll fluorescence phenotype, indicating substantial loss of chlorophyll and that absorbed light energy cannot be used efficiently, which is therefore dissipated as increased red chlorophyll fluorescence (Figure 4A). The T-DNA–induced *apo1* mutation of *Arabidopsis* was selected because it caused a complete loss of PSI activity (see below). Growth at 10 µmol photons m^{-2} s^{-1} was slower, but leaf morphology and development were unaltered in *apo1* in comparison to wild-type plants (Figure 4A). Under moderate light intensities of 50 µmol photons m^{-2} s^{-1}, mutant plants bleached rapidly, indicating increased light sensitivity.

2. Fluorometric and spectroscopic characteristics of the photosynthetic apparatus and pigment content in *apo1* revealed specific deficiencies of PSI

The light-induced *in vivo* chlorophyll fluorescence measurements can serve as a sensitive tool to estimate the excitation state of PSII reaction centres. The ratio of variable fluorescence to maximum fluorescence (Fv/Fm) reflects the potential capacity of the photochemical reaction of PSII (Krause and Weis, 1991). The fluorescence is quenched by the use of light energy (photochemical quenching [qP]) measured at intensities of 3 and 30 µmol photons m^{-2} s^{-1}. Fv/Fm reached levels of 0.62 ± 0.06 in *apo1* as compared with 0.81 ± 0.02 in the wild-type, indicating partial loss of PSII capacity or a stimulated emission of PSI antenna pigments that contribute to a higher minimum fluorescence with no effect on Fv. At the lower light regime, qP was reduced to 0.84 in the mutant as compared with 0.98 in the wild-type (Figure 4B).

At still moderate light intensities of 30 μmol photons m^{-2} s^{-1}, dramatic deficiencies were observed in qP processes in *apo1*. Whereas wild-type plants exhibited a qP of 0.81 under steady state conditions, *apo1* failed to quench most of the variable fluorescence (qP < 0.06; Figure 4B). Such a behaviour is typical for mutants affected in electron transport processes independent of PSII (Meurer et al., 1996a). This inference was confirmed by measuring the light-induced redox kinetics of the PSI pigment P700. Under normal conditions, P700 is completely reduced in the dark and oxidized to its maximum level in selective PSI light, whereas under steady state conditions in heterochromatic light, the P700 redox state is adjusted somewhere in between (Klughammer and Schreiber, 1994). Although the dual wavelength pulse amplitude - modulated system was set at maximal sensitivity, light-induced P700 redox changes were below the limit of detection in *apo1*, indicating complete loss of PSI function (data not shown). In plants grown heterotrophically, levels of chlorophylls were 10-fold reduced in *apo1* as compared with wild-type seedlings (1.84 ± 0.09 mg/g fresh weight in the wild type and 0.17 ± 0.03 mg/g fresh weight in mutants). The ratio of chlorophyll *a* to chlorophyll *b* was altered from 2.88 ± 0.04 in the wild-type to 2.64 ± 0.12 in the mutant. The photosynthetic pigment absorbance spectra demonstrated that the typical maxima at 430 and 670 nm for chlorophyll *a*, at 450 nm for chlorophyll *b*, and at 473 nm for carotenoids were present in the mutant (Figure 4C). The second derivative of the absorbance spectra showed a much broader carotenoid band at 473 nm in *apo1*, which is indicative of a relatively high carotenoid content and of an increased sensitivity to light (Figure 4C; Havaux and Niyogi, 1999).

3. Low-temperature fluorescence emission analysis demonstrates lack of the entire PSI complex in *apo1*

Fluorometric studies at 77K showed that the PSII-specific band at 685 nm was present in the mutant and not shifted to shorter wavelengths. This indicates that PSII reaction centers are present at normal levels relative to the outer light-harvesting complex II (LHCII) and that excitons can be efficiently transferred from LHCII to the inner PSII antenna (Krause and Weis, 1991). The usually most-abundant PSI-specific absorbance band at 735 nm was reduced to a hardly detectable shoulder in the spectra of *apo1* (Figure 4D). Therefore, it appears that PSII complexes are functionally assembled, whereas the whole PSI complex, including the outer antenna, severely and specifically fails to accumulate in *apo1*.
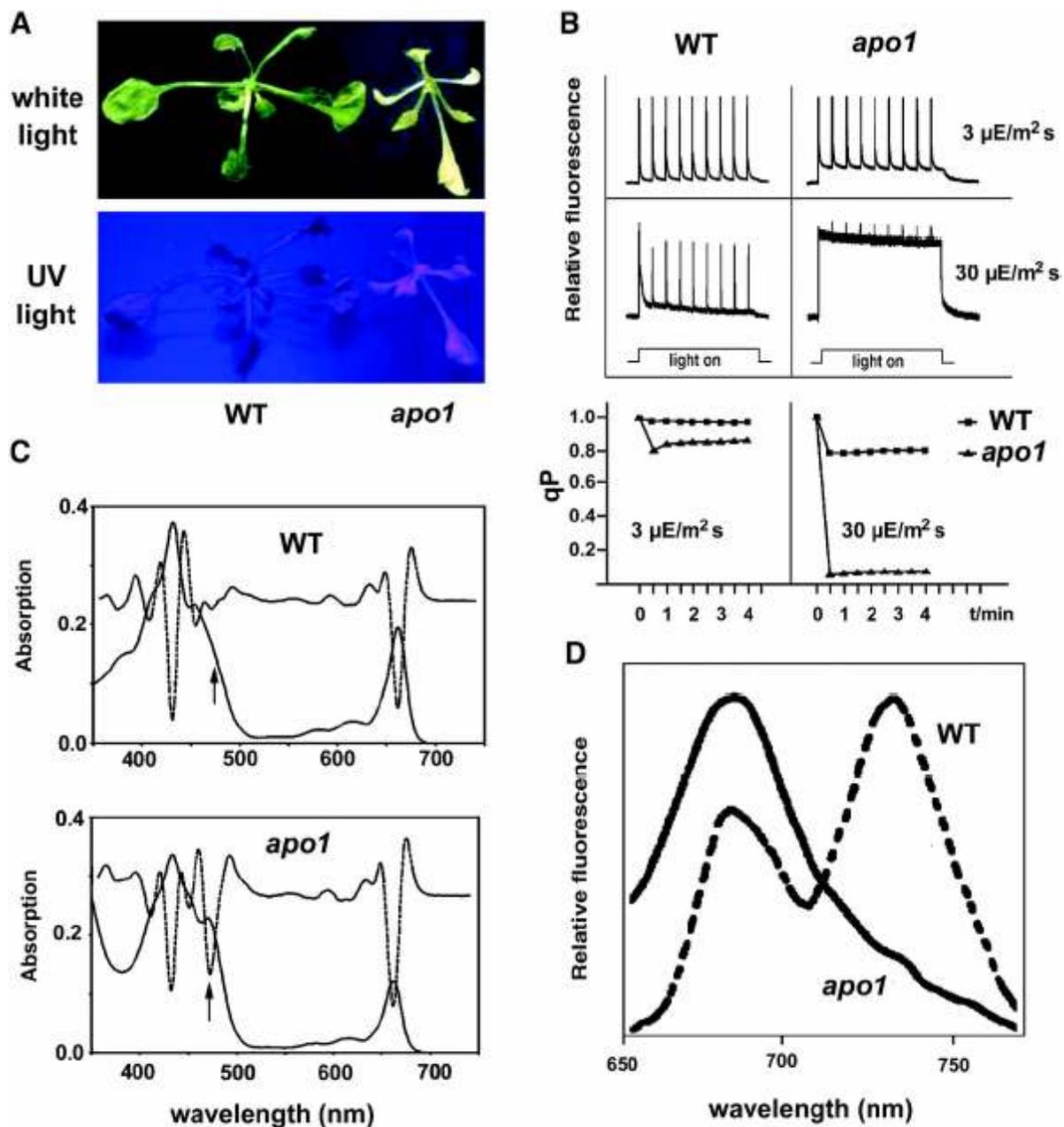
Figure 4: Phenotype, chlorophyll fluorescence, and absorbance spectra of *apo1* mutant plants.
(A) Three-week-old mutant plants growing on sucrose medium (MS medium) at 10 μmol photons m[-2] s^{-1} are pale and show a *hcf* phenotype under UV light. WT, wild-type.
(B) Chlorophyll fluorescence induction and qP at low (3 μmol photons m[-2] s^{-1}) and moderate (30 μmol photons m[-2] s^{-1}) light intensities. Leaves were exposed to a series of superimposed 800 ms saturating light flashes.
(C) Absorbance spectra of mutant and wild-type leaves grown at 10 μmol photons m[-2] s^{-1}. The increased band at 473 nm (see arrows) in the second order derivative spectra (dotted line) is indicative of an increased carotenoid accumulation in the mutant relative to chlorophyll levels.
(D) Low-temperature (77K) fluorescence emission spectra. The PSII band at 688 nm in the *apo1* mutant was normalized to the PSI band at 735 nm in the wild-type.

4. Intrinsic and peripheral PSI subunits are severely reduced in *apo1*

Stationary protein levels were normalized by equal loading of mutant and wild-type membrane and soluble proteins of the chloroplast. Immunological analysis of *apo1* revealed that nuclear-encoded and plastid-encoded proteins of PSII (subunits PsbB, PsbC, PsbD, and PsbO1/2) and cytochrome b_6f complex (subunits PetA and PetB) accumulated to significant levels between 50 and 100% (Figure 5A). Amounts of the ATP synthase (subunits AtpA and AtpG) and the soluble PetH and PetE proteins encoding ferredoxin-NADP reductase and plastocyanin, respectively, were unaltered in *apo1*. By contrast, only traces, if any, of the nuclear-encoded and plastid-encoded intrinsic PSI proteins PsaA/B, PsaC, PsaD, and PsaF could be detected in apo1 (Figure 5A). Levels of the peripheral antenna proteins of PSI were strongly reduced, amounting to 10% for LhcA1 and LhcA3 and 20% or less for LhcA2 and LhcA4 as compared with those of the wild-type (Figure 5B). This confirms the conclusions deduced from the 77K fluorescence data. The inability of *apo1* to accumulate significant amounts of the four antenna proteins of PSI contrasts findings with other known *Arabidopsis* PSI mutants because they are primarily and specifically affected in the accumulation of all core subunits but not to this extent of the outer antenna (Lezhneva and Meurer, 2004; Lezhneva et al., 2004). Remarkably, the outer PSII antenna proteins LhcB1 and LhcB2 were also significantly reduced to <20% of the wild-type (Figure 5B).

5. Accumulation of Fe-S cluster–containing proteins in *apo1*

Recent findings show that Fe-S cluster assembly is important for stable accumulation of PSI and other proteins or complexes within the chloroplast (Lezhneva et al., 2004; Touraine et al. 2004; Yabe et al., 2004). To investigate whether APO1 has additional targets that participate in chloroplast biogenesis, the accumulation of several plastid Fe-S cluster–containing complexes and proteins was studied (Figure 5C). Ferredoxin, which contains a [2Fe-2S] cluster, is not affected in size or in abundance in *apo1*. By contrast, the mutant had significantly reduced levels of [4Fe-4S] cluster–containing complexes like the ferredoxinthioredoxin reductase (FTR) and NAD(P)H-dependent dehydrogenase (NDH). The deficiency in accumulation of [4Fe-4S] clusters does not appear to be characteristic for mutants lacking PSI because *hcf*145, which is also missing the PSI core complex, shows

normal levels of other chloroplast [4Fe-4S] cluster proteins (Figure 5C; Lezhneva and Meurer, 2004; Lezhneva et al., 2004).
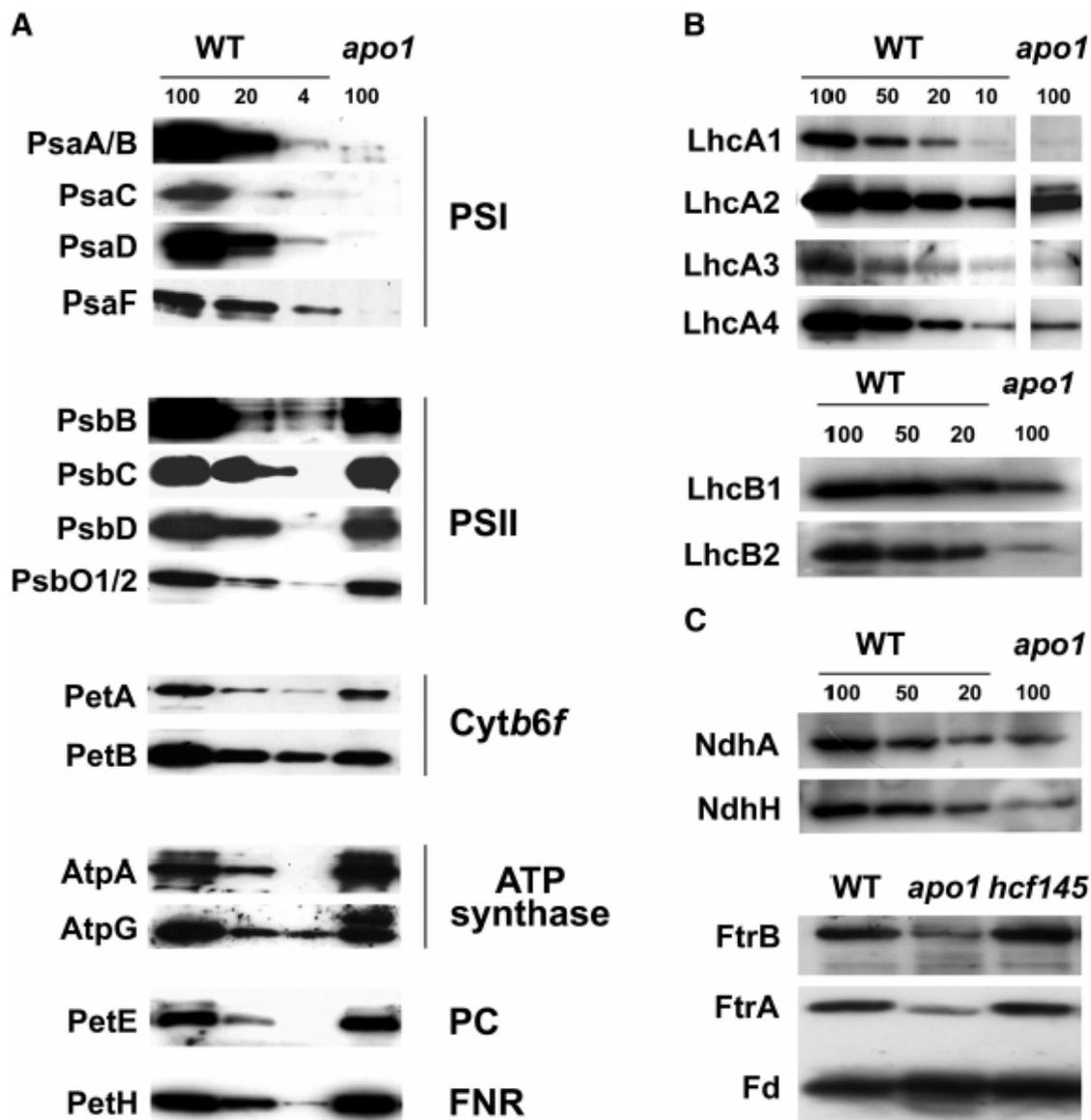

Figure 5: Accumulation of plastid proteins in wild-type and *apo1*.
Loading 100 corresponds to 8 μg of membrane or soluble proteins of the wild-type. The quantity of *apo1* thylakoid membranes (100%) was adjusted to wild-type levels of the ATP synthase. For quantification, dilution series of the wild-type were used. Three-week-old wild-type and *apo1* leaves were used for analysis.
(A) Immunoblot analysis of thylakoid membrane and soluble plastid proteins. Designations of proteins and of the corresponding complexes are labeled at the left and right, respectively.
(B) Immunoblot analysis of the outer PSI and PSII antenna proteins in apo1 and wild type. Lhc, Light-harvesting complex.
(C) Immunoblot analysis of Fe-S cluster–containing plastid proteins. The plastid-encoded thylakoid membrane and the nuclear-encoded soluble protein complexes NDH and FTR, respectively, contain [4Fe-4S] clusters. Ferredoxin (FD) binds [2Fe-2S] clusters.

6. Accumulation and integrity of PSI transcripts is unaffected in *apo1*

The abundance and sizes of nuclear (*psaD*, *psaE*, *psaF*, *psaG*, and *psaH*) and all plastid transcripts encoding PSI proteins (the trimeric *psaA-psaB-rps14*, *psaC*, *psaI*, and *psaJ*) were identical in mutant and wild-type plants as determined by RNA gel blot analysis and by expression profiling using macroarrays that were equipped with probes of all plastid genes (Figure 6A and data not shown). Transcript levels of the nuclear *cab* and *rbcS* genes, which are well known to be significantly reduced when the functional state of the chloroplast is arrested at an early stage (Surpin et al., 2002), were unaltered as well in *apo1* (Figure 6A). RNA gel blot analysis demonstrates that the *psaA-psaB* genes yield just a single prominent, tricistronic RNA of 5.3 kb in *Arabidopsis*. Primer extension studies uncovered that the transcript - terminus of the *psaA-psaB-rps14* tricistron is unaltered in *apo1* when compared with the wild-type (Figure 6B). This suggests that the *apo1* mutant exhibits normal promoter usage, integrity, and abundance of *psaA-psaB-rps14* transcripts.

7. Radiolabeling of the plastid PsaA and PsaB proteins is impaired in *apo1*

PSI protein abundance could be limited by translational disturbances in the mutant. Therefore, pulse labeling of membrane - bound and soluble chloroplast proteins was performed with [^{35}S]Met in the presence of the cytoplasmic translation inhibitor cycloheximide. With the exception of one plastid - encoded protein of 35 kD molecular mass, biosynthesis of other detectable soluble proteins in the stroma was unchanged in *apo1* (Figure 6C). Labeling of ATP synthase subunits α and ß (AtpA and AtpB) was slightly increased in the mutant relative to the wild-type control based on equal loading of radioactive label. Incorporation of radioactivity into the PSII proteins PsbA (D1) and PsbD (D2) was comparable to that in wild-type, but labeling of the chlorophyll binding proteins PsbB and PsbC was reduced. These data demonstrate the pleiotropy of the phenotype. As a control, the labeling pattern of *apo1* was compared with that of another *Arabidopsis* PSI mutant, *hcf*145, accumulating only 10% of the tricistronic *psaA-psaB-rps14* mRNA (Lezhneva and Meurer, 2004). The *hcf*145 mutant specifically exhibits decreased levels of PsaA and PsaB radiolabeling (Figure 6C) and, similar to *apo1*, increased incorporation of label into AtpA and AtpB. A failure to radiolabel the PSI

core proteins PsaA and PsaB in *apo1* could reflect that the rates of translation of the two PSI reaction center subunits are repressed in *apo1*. However, it also remains possible that the synthesis of PsaA and PsaB is unchanged in *apo1*, but the proteins or the nascent chains are rapidly degraded during the time course of the experiment.

8. Polysome association of p*saA* and *psaB* transcripts is decreased in *apo1*

If translation of *psaA* and *psaB* mRNAs is impaired in *apo1*, changes in polysome association for the *psaA* and *psaB* transcripts could be expected. Polysomal loading was analyzed by sucrose density gradient centrifugation. The sizes and distribution of polysomes loaded with *psaC* and *psbA* transcripts did not differ in the mutant when compared with the wild-type (Figure 6D). However, polysomes associated with tricistronic *psaA-psaB-rps14* transcripts were shifted to decreased sucrose concentrations, suggesting a failure in the functional loading of *psaA-psaB-rps14* transcripts with ribosomes in the mutant. To test whether initiation or elongation of translation is affected in *apo1*, the translation inhibitor lincomycin that prevents reinitiation and forces previously initiated ribosomes to run off was applied to wild-type and mutant plants 4 h before polysome isolation. As expected, the inhibitor caused banding of *psaApsaB-rps14* mRNAs at much lower sucrose concentrations in wild-type, whereas in *apo1* lincomycin induced a less prominent release of *psaA-psaB* transcripts from ribosomes, indicating that translational elongation is retarded in the mutant (Figure 6D).

Lincomycin treatment of the mutant was as effective as in the wild-type because *psbA*-containing and rRNA-containing polysomes were shifted towards the top of the gradient to the same extent in both cases. Therefore, it appears that APO1 is not needed for initiation but rather specifically for elongation of *psaA* and *psaB* translation, cofactor assembly during translation, or targeting of the nascent chains to their right place. However, the changes in the size of polysomes could also reflect an assembly mediated regulation of translation (Wostrikoff et al., 2004).
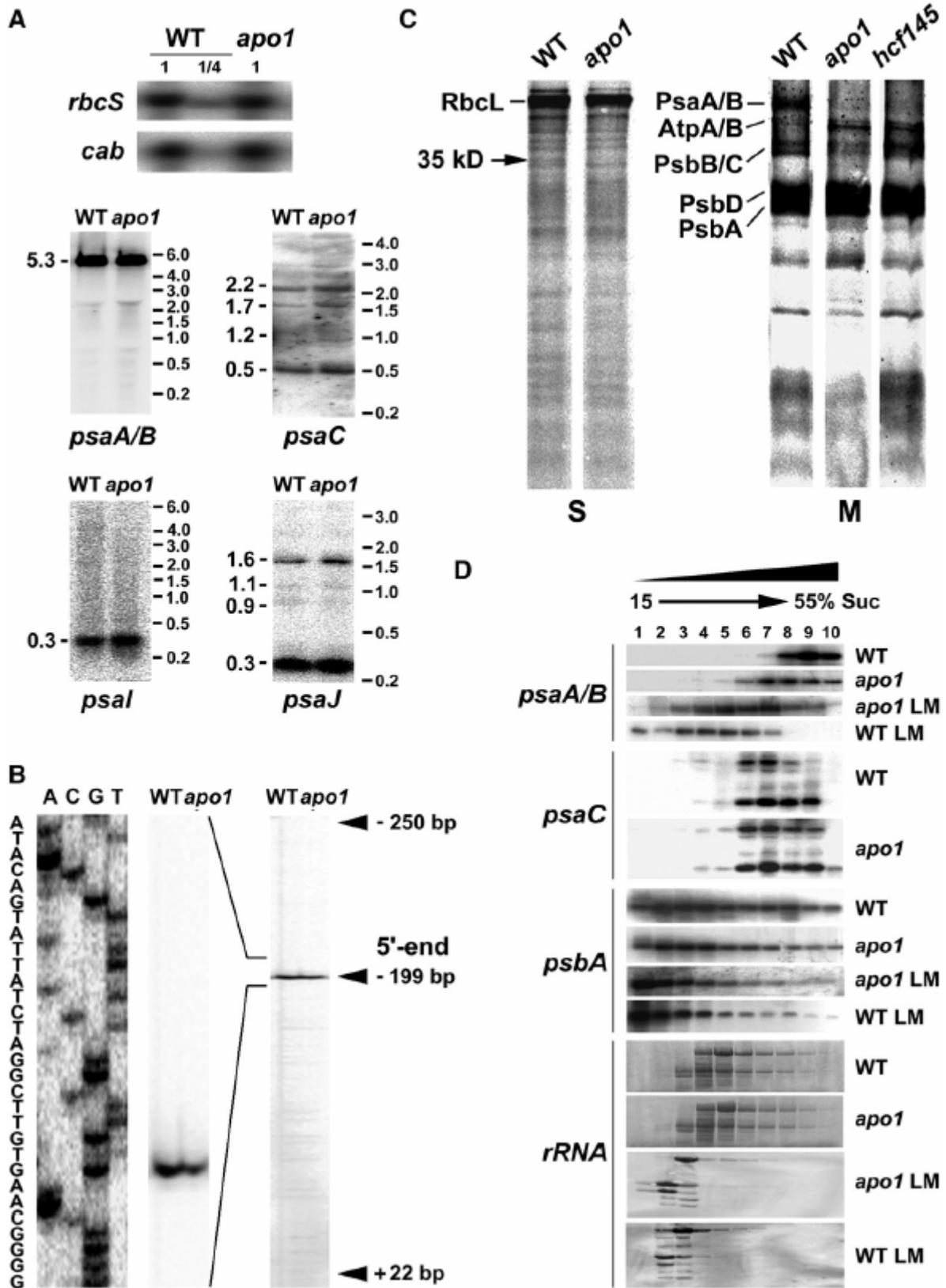
Figure 6: Quantities and integrity of *psaA-psaB* transcripts and protein labeling studies in wild-type and *apo1* mutant.
(A) RNA gel blot analysis of the plastid PSI genes and the nuclear *cab* and *rbcS* genes. Eight and two (1/4) mg of total RNA from three-week-old mutant and wild-type leaves were analyzed using gene-specific probes. Sizes of the standard (right) and the bands (left) are indicated in kilobases.
(B) Primer extension analysis of mutant and wild-type mRNA shows that the transcript 5` termini at position -199 nt relative to the start codon of the psaA message are intact in *apo1*.
(C) *In vivo* labeling of plastid soluble (S) and membrane (M) proteins separated by SDS-PAGE in *apo1*, *hcf145*, and the wild-type (WT). Wild-type and mutant proteins with equivalent amounts of radioactivity (100.000 cpm) were loaded.
(D) Polysome sedimentation in 15% to 55% sucrose (Suc) gradients by ultracentrifugation and subsequent RNA gel blot analysis of fractionated samples. Probes used are indicated on the left side. The filter used for the *psaC* probe was rehybridized with the *psaA-psaB* probe.
The filter of the lincomycin-treated (LM) material was used for *psaA-psaB* and re-hybridized with the *psbA* probe. Lincomycin treatment of wild-type and mutant plants was performed 4 h before polysome preparation. rRNAs have been detected by staining the blots.

9. Ultrastructure of *apo1* chloroplasts

The ultrastructure of *apo1* was compared with that of three other PSI-specific mutants, *hcf101*, *hcf140*, and *hcf113*, and of the wild-type (Figure 6). Wild-type chloroplasts showed a well developed membrane system consisting of interconnected grana and a random distribution of starch grains. The *apo1* plastids were 3 to 4 times smaller than those of the wild-type and appeared to be swollen. The mutant forms rudimentary thylakoids consisting only of stroma lamellae and fails to accumulate grana stacks. This indicates that membrane development is arrested at an early morphological stage and distinguishes *apo1* from other PSI mutants, which form larger (*hcf101*), swollen (*hcf140*), or unoriented (*hcf113*) grana stacks but only fragmentary stroma lamellae (Figure 7). The small size of the chloroplasts in *apo1* also explains the low level of chlorophyll based on the fresh weight.
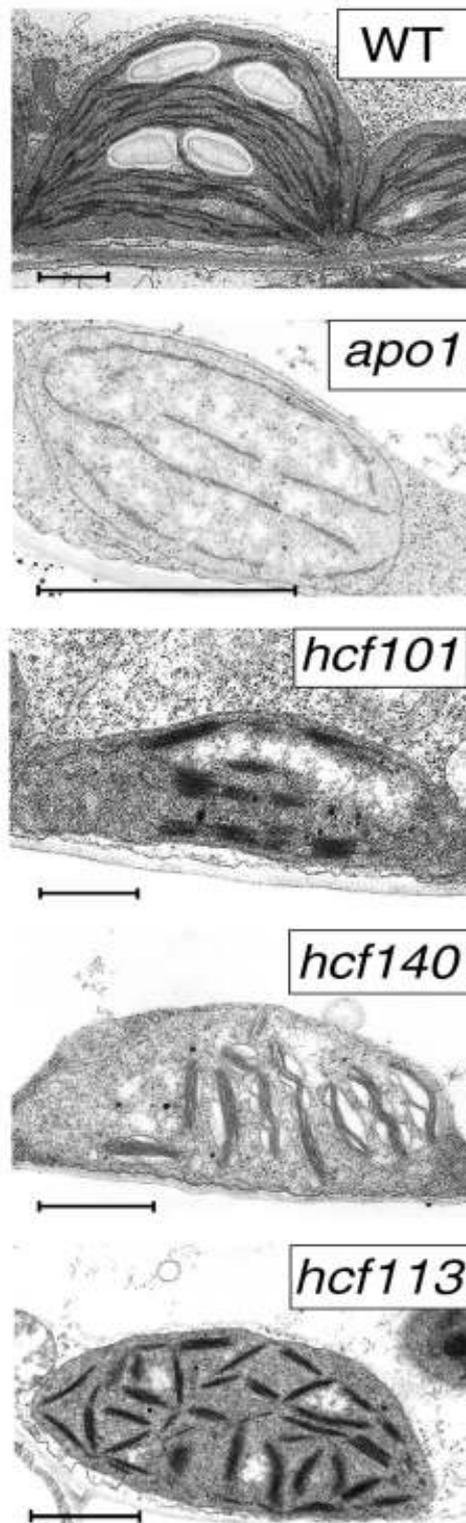
Figure 7: Chloroplast ultrastructure of the wild-ype and the PSI mutants *apo1*, *hcf101*, *hcf140*, and *hcf113*. Bars = 1 µm.

10. Molecular mapping, T-DNA tagging of *apo1* and complementation

The *apo1* mutation segregated in a Mendelian manner and was mapped between the two microsatellite markers nga128 and chr1-110 on the lower part of chromosome 1 at position 23.3956 ± 0.8 Mb. Neither known genes encoding plastid ribosomal proteins nor PSI genes map in this region (Legen et al., 2001), suggesting that APO1 encodes a novel protein. The kanamycin resistance conferred by the T-DNA cosegregated with the mutant phenotype in 384 analyzed segregants, indicating that APO1 is tagged by the insertion. The localization of APO1 to the lower part of chromosome 1 was confirmed by isolation and sequencing of the T-DNA left-border and right-border flanking regions by inverse PCR (Figure 8A). Using APO1 and T-DNA right-border probes for DNA gel blot analyses confirmed a single T-DNA insertion that cosegregates strictly with the *apo1* mutation (Figure 8B). The location of the insertion site close to the 5` end of APO1 at position 24.153 Mb of chromosome 1 (position p103 relative to the APO1 start codon) is consistent with the mapping data. The full-length cDNA of APO1 was isolated using a rapid amplification of cDNA ends (RACE) approach (Frohman et al., 1988). Interestingly, the APO1 start codon is localized in the second exon (Figure 8A). Expression of the full-length APO1 cDNA under the control of the 35S RNA Cauliflower mosaic virus promoter functionally complemented the mutant phenotype, resulting in the development of fully green seedlings which grew photoautotrophically and showed all physiological chlorophyll fluorescence and P700 redox characteristics which are typical for the wild-type (Figure 8C; data not shown).
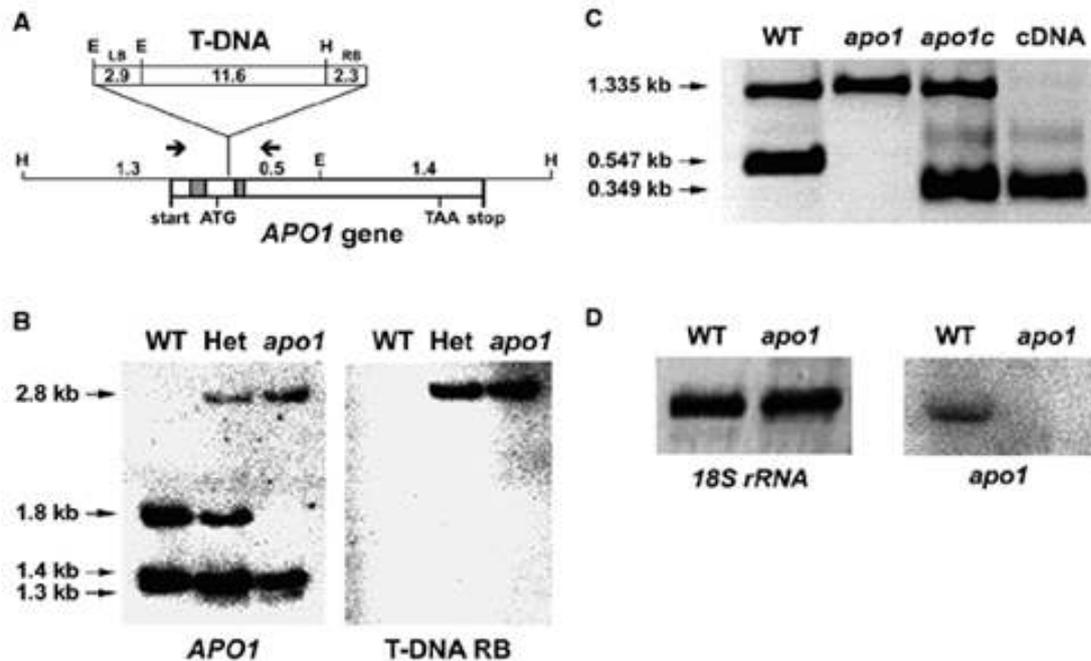
Figure 8: Inactivation of APO1 by T-DNA insertion and complementation of *apo1*.
(A) Schematic view of the T-DNA insertion in *apo1*. The two introns are indicated by shaded boxes. HindIII (H) and EcoRI (E) restriction sites and the T-DNA left (LB) and right (RB) borders are shown. Sizes are given in kilobases. The transcription start and stop are indicated. The arrows show the positions of primers used in (C). The position of the translational start (ATG) and stop (TAA) codons are indicated.
(B) Genomic DNA gel blot analysis of EcoRI and HindIII double-digested mutant and wild-type (WT) DNA results in polymorphisms that can be deduced from (A). The probes used of the T-DNA right border (RB) and the APO1 gene recognize one and the same 2.8-kb fragment. Het, heterozygous plants for *apo1*.
(C) PCR analysis of wild-type, mutant, complemented mutant lines (*apo1c*), and the *apo1* cDNA. Control primers, which amplify another chromosomal region of 1.335 kb, were used in the same reaction with the APO1 gene-specific primers. APO1 exon-specific primers *apo* 1-f and *apo*1-r2 did not amplify a 0.547 kb product of genomic DNA in the a*po1* mutant and complemented lines, but a 0.349 kb fragment originating from the expressed cDNA.
(D) RNA gel blot analysis of mutant and wild type (WT) was performed with a probe specific for *apo1*. Equal loading (8 mg) is shown by hybridization with a probe specific for 18S rDNA.

11. Expression of *apo1* is stimulated in illuminated leaves

APO1 transcripts of 1.65 kb could be detected in the wild-type but were absent in *apo1*, consistent with the T-DNA insertional inactivation of the APO1 gene (Figure 8D). Because transcript abundance of APO1 was very low even in the wild-type, the precise expression levels of APO1 were estimated by real-time RT-PCR using 18S rRNA for normalization. Twelve-day-old dark-grown wild-type seedlings expressed 23% ± 5% of the light control. Expression in roots, stems, siliques, and flowers was 28% ± 3%, 63% ± 6%, 23% ± 4%, and 69% ± 6%, respectively, relative to that found in leaves. Although substantial transcript levels were already present in the dark and in roots, expression of *apo1* appears to be stimulated during photomorphogenesis. This implies an important role of APO1 in the dark as well as in non - photosynthetic tissues.

12. Localization of APO1 to plastid nucleoids

In vitro synthesized APO1 precursor proteins of 49 kD were imported into chloroplasts and processed to a mature size of 42 kD (Figure 9A), demonstrating the presence of a cleavable transit peptide even if no chloroplast target sequence could be identified with any of the prediction programs available in public databases. To sublocalize APO1 within the chloroplast, the APO1 cDNA was translationally linked to the gene for green fluorescent protein (GFP) and transiently expressed in isolated protoplasts. The green fluorescence was found exclusively in chloroplasts consistent with the findings of the *in organello* experiments (Figure 9B). Although there is a diffuse GFP signal apparently throughout the stroma, much of the APO1-GFP fusion resided in distinct spots within the organelle. Comparing the fluorescence induced by GFP with that induced by 4'-6-diamidino-2-phenylindole (DAPI) - stained cells indicates that the fluorescent labels of both samples overlapped. Therefore, APO1 appears to be associated with plastid nucleoids (Figure 9B). The relative intensity of the APO1 - GFP and DAPI fluorescence varied in the individual spots, indicating that APO1 has a higher affinity to a distinct fraction of nucleoids. It is important to note that APO1-GFP association with nucleoids does not seem to reflect an unspecific aggregation of over-

expressed protein because the compartmentalization was also apparent in chloroplasts with barely detectable APO1 - GFP fluorescence and not observed with other highly expressed chloroplast-targeted GFP fusions which showed a uniform distribution (Meurer et al., 1998a).

13. APO1 belongs to a novel gene family in vascular plants with four defined groups containing a conserved repeat motif

The APO1 gene encodes a previously unknown protein and shows similarities to genes only found in vascular plants (Figure 10; data not shown). The absence of similarities in the sequenced genomes of eubacteria, archaebacteria, or *Chlamydomonas* indicates that the APO gene family evolved after the divergence of the green lineage or has been lost in related lineages. Using public databases (http://bioinf.cs.ucl.ac.uk/psipred/; http:// us.expasy.org), all attempts to identify sequence motifs or domains within APO1 that are indicative of a function failed. Because the instability index of APO1 is computed to be 44.97, the protein is classified to be unstable (Guruprasad et al., 1990). According to structural predictions, APO1 consists of extensive random coiled (58%) and, to a lesser extent, of alpha helical (28%) and extended strand (14%) structures. At the theoretical pI of 9.27 the APO1 protein contains 436 amino acid residues and has a deduced molecular mass of 49.6 kD consistent with the size of *in vitro* translated APO1 proteins (Figures 9A and 10A).
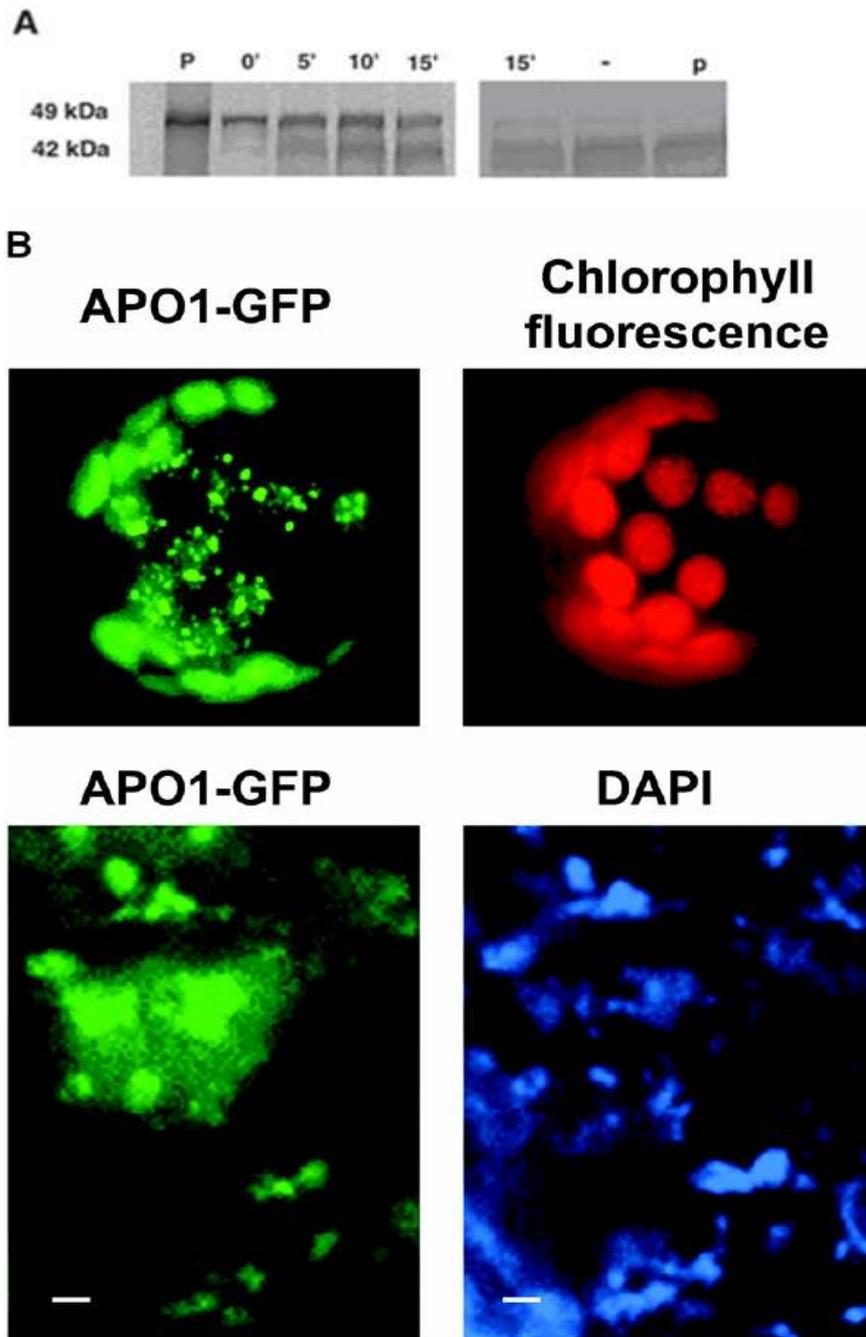
Figure 9: Localization of APO1 within the chloroplast.
(A) Import of radiolabeled APO1 proteins into isolated chloroplasts and subsequent detection of gel-separated proteins by phosphor imaging. The precursor of 49 kD (P) was imported and proteolytically processed to 42 kD at the indicated periods of chloroplast incubation. After import chloroplasts were either treated (p) or not treated (-) with thermolysin to digest not - imported proteins.
(B) The APO1 protein was fused to GFP (APO1-GFP) and transiently expressed in tobacco protoplasts. GFP fluorescence was exclusively found in spots inside the chloroplast as revealed by chlorophyll fluorescence (top). Transformed protoplasts were incubated with DAPI and visualized at higher magnification (bottom). Bars = 1μm
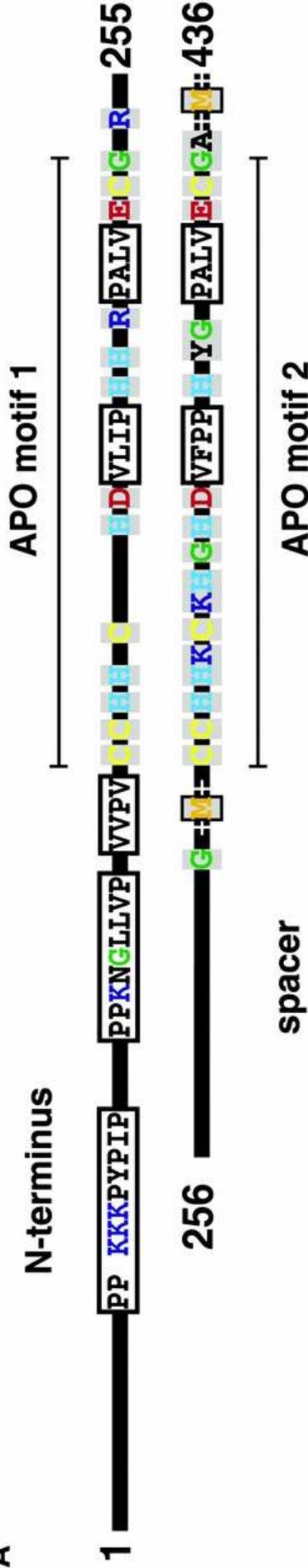
Three additional homologous genes of unknown function, APO2 to APO4, are present in the *Arabidopsis* genome. Interestingly, each of the four APO proteins possesses an orthologous counterpart in the rice genome (Figure 10B). Therefore, the APO gene family consists of four distinguishable groups that are present in both monocotyledonae and dicotyledonae. APO1 to APO4 show much fewer similarities in the N terminus than in the remaining part of the proteins, indicating different localizations and/or functions. APO2 is also predicted to be localized in the chloroplast. In rice (*Oryza sativa*), APO3 is computed to be present in the chloroplast as well, whereas the *Arabidopsis* protein is predicted to be localized in mitochondria. APO4 is computed to represent a mitochondrial protein in both organisms. All members of the previously unknown APO gene family contain a 100 amino acid residues - spanning region (APO motif 1) with conserved Cys, His, Gly, and acidic and basic amino acids (Figure 10). The highly conserved APO motif 1 is duplicated at the C terminus (designated APO motif 2). These two motifs are always separated from each other by a less-conserved spacer that is also variable in length but in groups 1 to 3 contains one conserved Met embedded within positively charged amino acid residues directly upstream of APO motif 2 (Figure 10). A similar sequence is also present downstream of APO motif 2 close to the C terminus in all groups. APO motif 1 is followed by a short stretch containing positive charges in groups 1 to 3. The highly conserved signature of both motifs in APO1, which fits to all members of the APO gene family in vascular plants, can be defined as C-x2-C-x3-(H,Q)-x4-GH-x4-C-x11-H-x-W-x6-D-x8- H-x(20-26)-PA-x2-E(L,I)C-x3-G. The conserved Cys in both motifs could provide ligands for tetranuclear Fe-S centers (Sticht and Rösch, 1998). Several conserved differences between the two motifs could indicate different functions (Figure 10B). For example, both motifs, APO 1 and 2, contain a conserved H in another position. Two conserved R residues are present in APO motif 1 and two K residues in motif 2. In addition, APO motif 2 contains conserved G, VW, YG, and A residues, which are not present in APO motif 1 in any of the groups (Figure 10).

Figure 10: Sequence analysis of the APO gene family in *Arabidopsis* and rice.
(A) Scheme of the primary APO1 structure with the conserved and repeated APO motifs 1 and 2. Conserved amino acid residues in group 1 and differences between motifs 1 and 2 present in this group are highlighted.
(B) Sequence alignment of motifs 1 and 2 in APO1 to APO4 in Arabidopsis (At) and rice (Os). Amino acid residues that are conserved in all members are on gray background. Amino acid residues that are specific for each defined group in *Arabidopsis* and rice and different in the others are underlined. Conserved differences between the motifs 1 and 2 in all four groups are listed below the alignment.

Part B: Characterisation of the psaJ gene

14. Targeted inactivation of the tobacco chloroplast *psaJ* gene

PsaJ is a subunit of PSI in almost all photosynthetic organisms studied so far; the unicellular cyanobacterium *Gloeobacter violaceus* PCC 7421 appears to have a PSI without PsaJ (Nakamura et al., 2003; Inoue et al., 2004). PsaJ in higher plants is a protein of 44 amino acid residues, consisting of one membrane-spanning helix that is highly hydrophobic (Fig. 11). To determine the function of psaJ in plants we have taken a reverse genetics approach and constructed a knock - out allele for targeted disruption of the tobacco *psaJ* (Fig. 12A). The knock - out allele was introduced into the tobacco plastid genome by particle bombardment-mediated chloroplast transformation (Svab and Maliga, 1993).


```
PSAJ_ARATH   -MR-DLKTYLSVAPVLSTLWFGSLAGLLIEINRLFPDALTFPFFSF    44
PSAJ_TOBAC   -MR-DLKTYLSVAPVLSTLWFGALAGLLIEINRFFPDALTFPFFSF    44

PSAJ_CHLRE   -MK-DFTTYLSTAPVIATIWFTFTAGLLIEINRYFPDPLVFSF---    41
PSAJ_PORPU   -MNNNFTKYLSTAPVIGVLWMTFTAGFIIELNRFFPDVLYFYL---    42

PSAJ_SYNEL   -MK-HFLTYLSTAPVLAAIWMTITAGILIEFNRFYPDLLFHPL---    41
PSAJ_PROMA   MFKIFSTKWFRSAPVVATIWIVITAGILVEWNRFVPDLLFHPGL--    44
             :.      .::  ***:...:*:   **::* ** ** *
```
Transmembrane span

Figure 11: Alignment of PsaJ sequences representing cyanobacteria, algae and higher plants. In the database there are a total of 47 full-length PSI-J sequences and all were aligned using Clustal W. In the alignment shown are the sequences from plants (*A. thaliana* and tobacco), algae (*Chlamydomonas reinhardtii* (CHLRE) and *Porphyra purpurea* (PORPU)) and cyanobacteria (*Synechcoccus elongatus* (SYNEL) and *Prochlorococcus marinus* (PROMA)). Amino acid residues involved in Chl binding (W (Trp), E (Glu) and H (His) are shown in green *. Note that the histidine residue is only conserved in cyanobacteria in agreement with the notion that PsaJ of cyanobacteria is involved in binding 3 Chls whereas plant PsaJ only binds two Chls. Amino acid residues contacting β-carotene (I (Ile) and R (Arg) are indicated in red *.

From 10 bombarded leaf samples 19 chloroplast transformants were selected as verified by PCR and DNA gel blot analysis. (Fig. 12B). Two independent transplastomic lines were subjected to additional rounds of regeneration on spectinomycin-containing medium to obtain homoplastomic tissue.
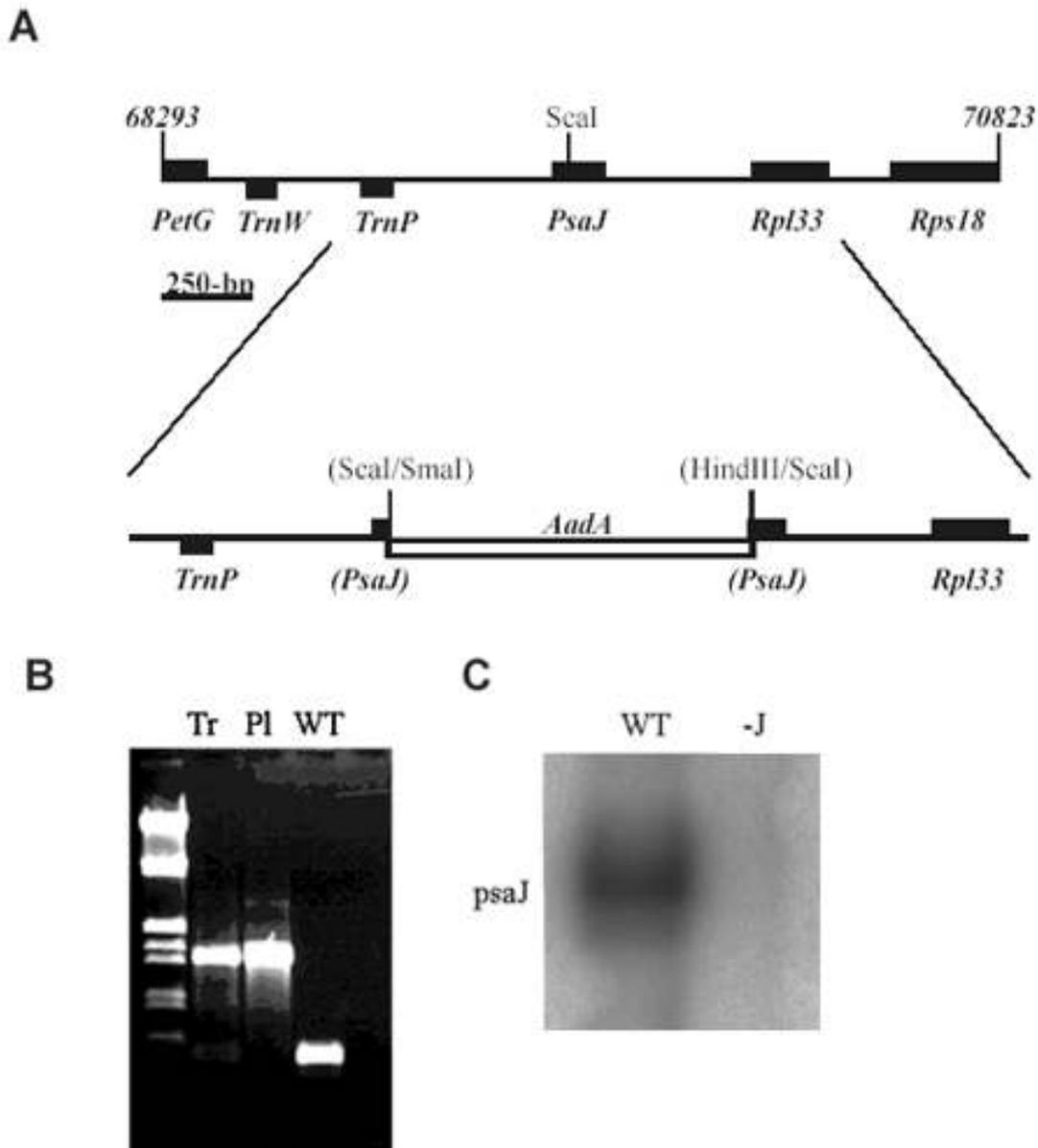
Figure 12:
(A) Construction of the plastid transformation vector. Schematic map of the 2.53 kb chloroplast genomic fragment containing the *psaJ* gene. The a*adA* cassette is inserted into a ScaI site within the coding sequence of psaJ in the sense orientation.
(B) PCR confirmation that the *aadA* insert is in the *psaJ* gene:
Primers used for amplification: psaj-f.: 5´-TCGGTAAGAAAGAAGGGGATG-3´ and psaj-r.: 5´-CAGTTAATTCGAACTTGAGC-3´. λ-DNA digested with EcoRI/HindIIIis used as length standard. Left lane: Transformed plants (Tr); middle lane: plasmid of the transformation vector (Pl, Fig. 2A); right lane: wildtype tobacco plants (Wt)
(C) Northern blot showing that there is no psaJ messenger RNA.

15. Plants devoid of PsaJ are affected in photosynthetic performance

When plants lacking PsaJ were transferred to soil they grew photoautotrophically and were fully fertile (Fig. 13). The original transformed lines were self-pollinated, and the seeds produced were germinated directly on soil. The resulting offspring displayed the same characteristics as the first generation.
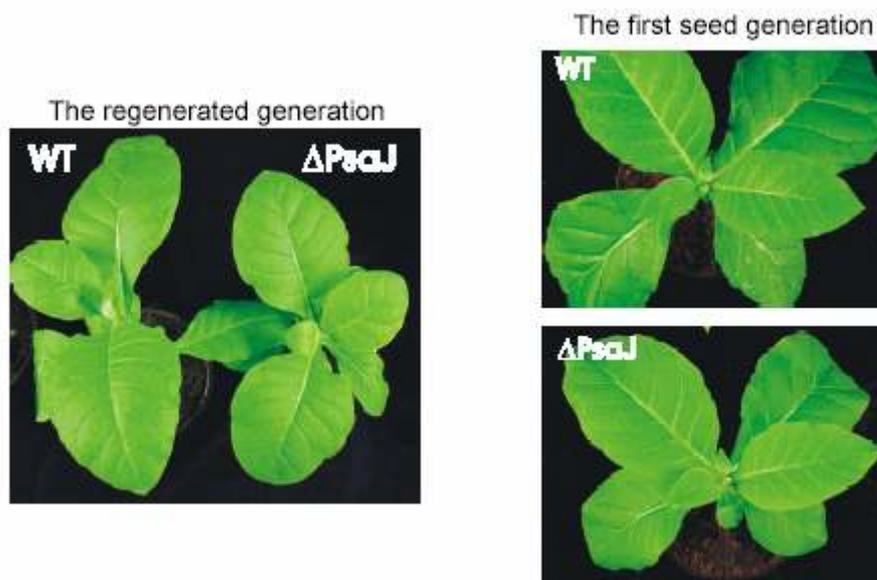
Figure 13: Phenotype of homoplastomic $\Delta psaJ$ plants grown under growth chamber conditions.
(A) Photograph of plants from the regenerated generation.
(B) Photographs of individual plants from the first seed generation. Note that the $\Delta psaJ$ plants are slightly smaller and also slightly paler than the wildtype plants.

Tobacco plants lacking PsaJ were slightly smaller than wild-type plants. This was observed for both growth-chamber and green-house grown plants and suggests that elimination of the PsaJ protein from PSI affects the photosynthetic performance.

Besides being slightly smaller than wild-type, the *psaJ* knock-out plants were also visibly paler. Pigment extraction of leaf disks using boiling ethanol and spectrophotometric quantification showed a 13% reduction in the content of chlorophylls per leaf area when compared to wild-type (Figure 14).
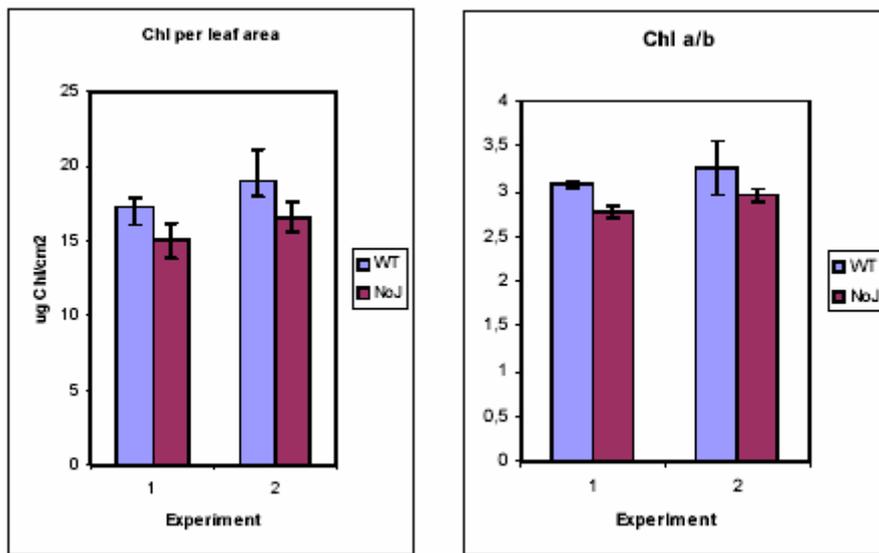
Figure 14: Chlorophyll measurements: Estimated from the leaf extracts the Chl *a*/*b* ratio was 2.95 in the *psaJ* knock-out leaves compared to 3.25 in those of wild-type. This difference was caused by a larger decrease in Chl *a* (15% less) and only a small decrease in Chl *b* (6% less) in the mutant. Similar measurements on several independent preparations of thylakoids also revealed a smaller Chl *a*/*b* ratio in the mutant although the absolute numbers were different. In thylakoids from PsaJ-less plants the Chl *a*/*b* ratio was 2.50, whereas in wild-type plants the ratio was 2.73. Thus, the reduced Chl *a*/*b* ratio in the absence of PsaJ suggests that plants without PsaJ either have a lower PSI/PSII ratio or an increase in the Chl *b* containing peripheral antenna.

To analyze this finding further the amount of P700 was determined in solubilized thylakoids using chemical oxidation and reduction of P700. The number of chlorophylls/P700 reaction centre was 490 ± 43 for wild-type and 684 ± 99 for thylakoids from the PsaJ-less plants (Figure 15). Based on these data the increased Chl/P700 ratio corresponds to approximately 35 - 40% less PSI in plants lacking PsaJ. A reduction in the amount of PSI relative to PSII should result in an imbalance in the linear electron flow. The PSII excitation pressure (estimated as $1-q_P$) was therefore measured directly in the growth chamber under those light conditions to which the plants were adapted. Under these conditions $1-q_P$ was increased 1.7-fold in the plants lacking PsaJ (Figure 15) indicating that the PSII excitation pressure was significantly increased due to a more reduced plastoquinone pool. Measuring $1-q_P$ under greenhouse conditions on either a cloudy or a sunny day confirmed the higher excitation pressure in plants without PsaJ and especially under conditions where the plants have to cope with higher light intensities. This is in agreement with a restriction of electron flow at PSI.

At the same time the photochemical efficiency of photosystem II (Φ_{PSII}) was reduced by 10% compared with wild type.
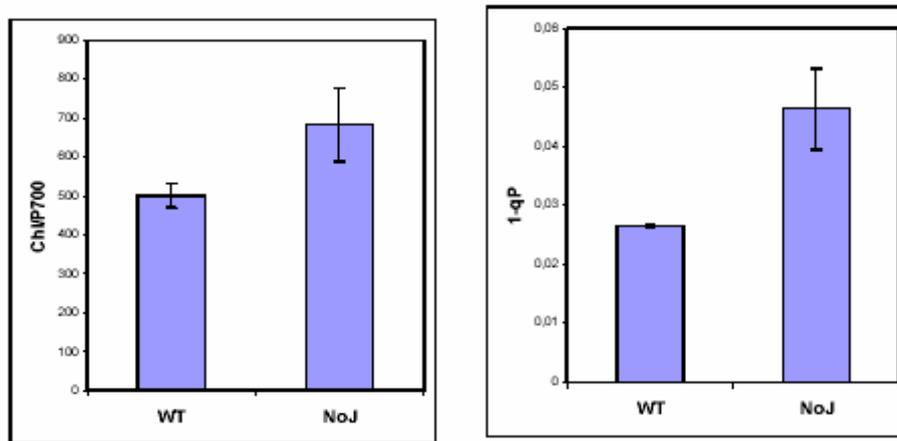
Figure 15: Number of chlorophylls/P700 (left) and PSII excitation pressure (right) in wild-type and *psa*J mutant. Chl/P700: The number of chlorophylls/P700 reaction centre was 490 ± 43 for wild-type and 684 ± 99 for thylakoids from the PsaJ-less plants, these data result in an decrease of PSI ofapproximately 35 - 40% in plants lacking PsaJ. The PSII excitation pressure (estimated as 1-q$_P$) was measured under growth light conditions and shows a 1-q$_P$ – value that was increased ≈1.7-fold in the plants lacking PsaJ.

16. The amounts of PSI core subunits are significantly reduced in the absence of PSI-J

The estimation of Chl per P700 indicated that there is less PSI in the Δ*psaJ* plants. In order to visualize this by an independent method and also to analyze whether the absence of PsaJ caused changes in other major thylakoid complexes immunoblot analysis of thylakoid proteins was performed using a variety of antibodies directed against subunits of the PSI-, PSII-, Cytb_6f- and ATP synthase complexes (Figure 16). The gels were loaded with proteins corresponding to equal amounts of chlorophyll. This analysis showed that subunits of PSII, of the Cytb_6f complex and of the ATP synthase were present in amounts close to the amounts found in wild-type (Fig. 16A). In contrast, the amounts of all analysed subunits of the PSI core were consistently reduced by approximately 50% compared to wild-type (Fig. 16A). This strongly suggests that PsaJ is required for stable accumulation of PSI either due to a requirement of the subunit for assembly or stability of the PSI complex.

A)

WT   NoJ   WT   NoJ   WT   NoJ

1 0.5 0.25 1 0.5   1 0.5 0.25 1 0.5   1 0.5 0.25 1 0.5

B)
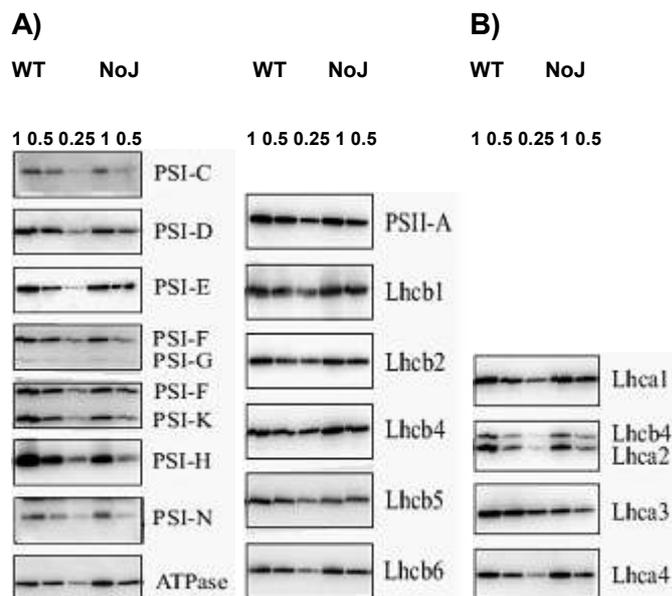
Figure 16: Immunoblot analysis of proteins in thylakoids prepared from Δ*psaJ* and wild-type plants.
(A) Content of a range of PSI core proteins and representative PSII proteins in Δ*psaJ*. Thylakoids were prepared from leaves from 2 - 4 different wild-type or Δ*psaJ* plants. A dilution series containing protein corresponding to 0.25, 0.5 and 1.0 μg chlorophyll of the wildtype and 0.5 to 1.0 μg chlorophyll of the mutant was separated by SDS-PAGE, blotted and analyzed with the antibodies indicated. WT and Δ*psaJ* dilutions were run side by side and for each antibody the resulting signal was quantified using the LabWorks software as described in the material and methods. The figure shows only the dilutions that gave a linear response, i.e. doubling in loaded protein should result in a doubling of measured signal.
(B) Content of light harvesting chlorophyll *a/b* proteins of PSI and PSII. Thylakoid proteins were separated as above and the blots were incubated with antibodies as indicated. The Lhca2 antibody also detects Lhcb4 (CP29). Quantification was performed on two independent preparations of both WT and Δ*psaJ* thylakoids.

The Lhca proteins, which constitute the peripheral antenna of PSI, were not reduced to the same extent as the core subunits. Lhca1 and Lhca4 are present in near wild-type amounts, and Lhca2 and Lhca3 are reduced by 10 - 20% compared to wild-type. This clearly indicates that the Lhca proteins are present in excess of the PSI core complexes and most probably accumulate unassembled in the membrane. In order to investigate this further fluorescence emission was measured at low temperature. Fluorescence emission spectra between 650 and 800 nm during excitation at 435 nm at 77 K using intact leaves of wild-type plants and plants devoid of PsaJ are shown in Fig. 17. The spectra revealed that in the absence of PsaJ there is a 2 - 3 nm blue shift in the far red emission originating from PSI-LHCI. Furthermore, the ratio between the far red emission and the PSII emission at 685 nm is decreased which is in agreement with the decreased content of PSI in the absence of PsaJ. The blue shift suggests a perturbation of the peripheral antenna, which either is because PsaJ plays a functional role in the binding/function of the LHCI antenna or because unassembled Lhca complexes are present in the membrane.
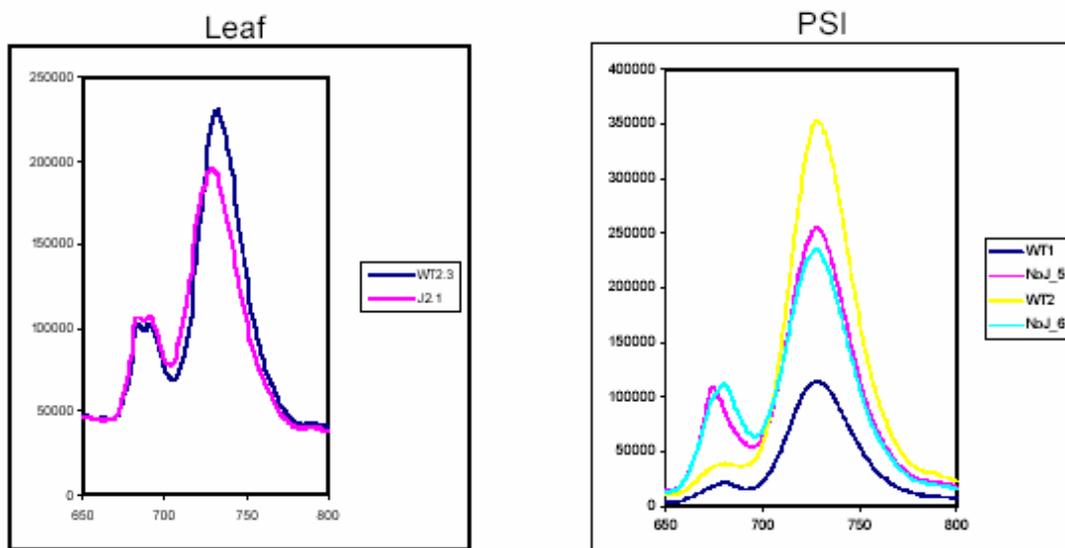
Figure 17: Low temperature fluorescence emission. Shown are the spectra of intact leaves from a wild-type plant (WT) and a Δ*psaJ* plant (Δ*psaJ*). Leaves from several individual plants of both genotypes were measured and the mutant consistently showed at least a 2 nm blue shift in the far-red fluorescence emission peak. Excitation wavelength was 435 nm.

The latter possibility was tested by gentle solubilization of the various thylakoid membrane complexes using N-dodecyl-β-D-maltoside and subsequent separation of the complexes using sucrose gradients. After separation the gradients were harvested in 0.5 ml fractions and the individual fractions were analysed by gel electrophoresis and immunoblotting analysis using antibodies against the four Lhca proteins and selected PSI subunits (Figure 18). This analysis revealed that significant amounts of free Lhca proteins were found in the fractions where normally free Lhc-complexes – mainly LHCII trimers and/or Lhcb-monomers – normally are found.
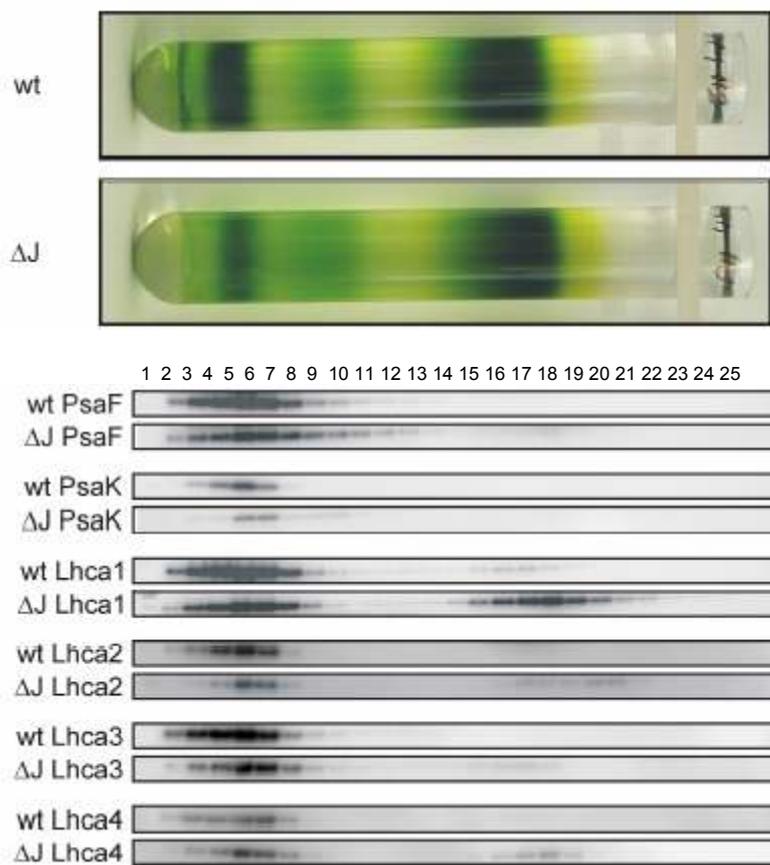
Figure 18: Western analysis of LhcA-proteins: Solubilised thylakoid membrane complexes (with N-dodecyl-β-D-maltoside) were separated using sucrose gradients. Afterwards gradients were harvested in 0.5 ml fractions and the fractions were analysed by gel electrophoresis and immunoblotting analysis using antibodies against the four Lhca proteins and PsaK as well as PsaF.

To find out whether the excess Lhca antenna proteins were functionally attached to the PSI complexes we estimated the functional antenna size of PSI using light-induced P700 absorption changes at 810 nm after very gentle solubilization of the thylakoid membrane using digitonin as described in the section Materials and Methods. This method was previously used to successfully detect changes in PSI antenna due to association with LHCII during state transitions (Zhang and Scheller, 2004) or due to genetic elimination of individual Lhca proteins in *Arabidopsis* (Klimmek et al., 2005). The functional PSI antenna size was estimated as the $t_{1/2}$ value which is defined as the time it takes to oxidize 50% of the P700 in the sample and was estimated at three different intensities of actinic light. At all three light intensities there was no difference in the $t_{1/2}$ value in the samples lacking PsaJ when compared to the values obtained with wild-type samples (Figure 19) suggesting that the PSI antenna size is unaffected by the elimination of PsaJ and furthermore rule out that PsaJ is strictly required for binding of any of the Lhca antenna proteins.
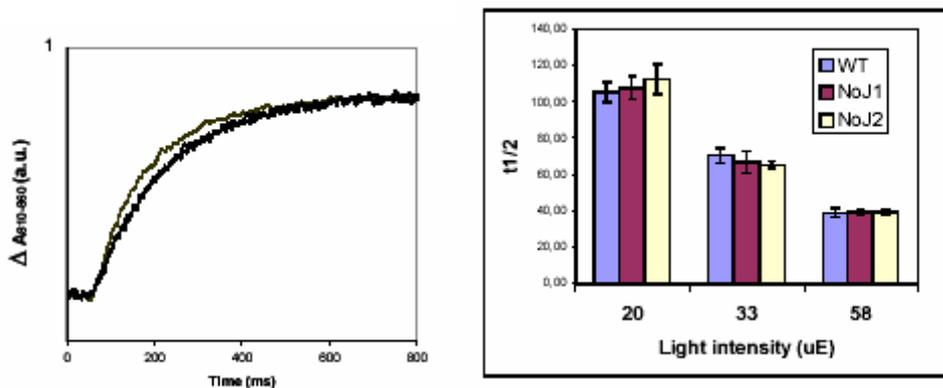
Figure 19: Measurement of PSI antenna size: The functional PSI antenna size was estimated as the $t_{1/2}$ value (defined as time to oxidize 50% of the P700 in a sample) at three different intensities of actinic light. No differences between wild-type samples and mutant material was observed.

17. PsaJ does not affect interaction with plastocyanin

Based on work with *Chlamydomonas* mutants lacking PsaJ it has been proposed that the function of PSI-J is to maintain PSI-F in a proper orientation which allows fast electron transfer from PC or Cyt c_6 (Fischer et al., 1999). A similar role of PsaJ in higher plants is likely and in order to analyse this, NADP$^+$ photoreduction was determined using thylakoids purified from plants without PSI-J and wild-type plants. In the standard assay with 2 μM

plastocyanin an activity of 11.9 ± 0.6 µmol of NADPH s^{-1} (µmol of P700)$^{-1}$ ($\pm$ S.D., n = 6) was obtained with thylakoids from wild-type. With thylakoids devoid of PSI-J an activity of 4.9 ± 0.4 µmol of NADPH s^{-1} (µmol of P700)$^{-1}$ ($\pm$ S.D., n = 6) was determined. Thus, in the absence of PsaJ PSI has a 50 - 60% slower rate of *in vitro* NADP$^+$ photoreduction. At varying concentrations of PC a similar difference in activity between wild-type and ΔPsaJ was seen (Fig. 20).
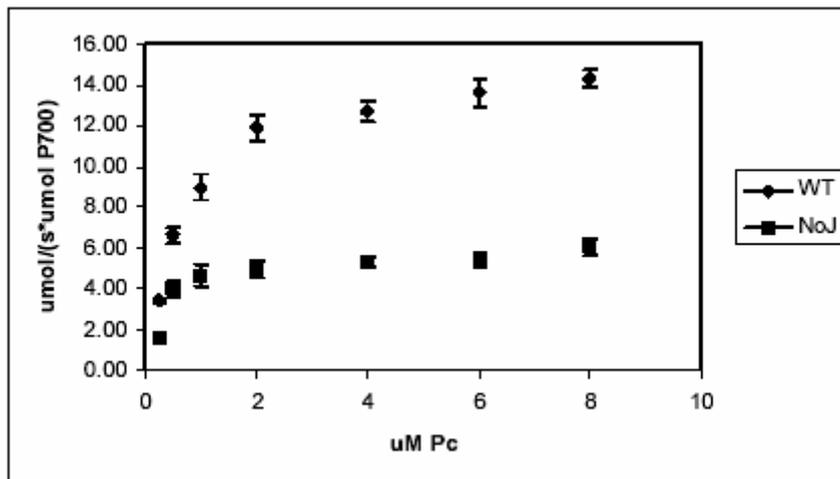
Figure 20: NADP$^+$ photoreduction measurements: NADP$^+$ photoreduction was determined at varying concentrations of PC using thylakoids purified from plants without PSI-J and wild-type plants. In the absence of PsaJ PSI shows a 50 - 60% decreased rate of *in vitro* NADP$^+$ photoreduction.

The results from the *in vitro* NADP$^+$ photoreduction measurements clearly indicated that PsaJ somehow affects electron transport. The work with green algae had suggested that the most obvious step was the electron transfer from PC to PSI (Fischer et al., 1999). This reaction is a multi-step reaction, which can be divided into three major steps: binding of PC to P700, electron transfer within a complex between PC and P700, and release of oxidized PC from the complex between PC and P700 (Hippler et al., 1996). To investigate the kinetics of the PC-PSI interaction, flash-induced P700 absorption transients were determined by following the absorption at 820 - 835 nm in the presence of varying concentrations of PC ranging from 0 to 500 µM (Bottin and Mathis, 1985; Nordling et al., 1991; Sigfriedsson et al., 1996). Flash excitation of PSI results in a very rapid absorption increase at 834 nm due to photo-oxidation of P700, followed by a slower absorption decrease due to reduction of P700$^+$ by PC.

The P700 absorption decrease can be modelled as the sum of three exponential decays discerned as a fast phase, an intermediate phase and a slow phase (Bottin and Mathis, 1985; Nordling et al., 1991; Sigfriedsson et al., 1996). The data obtained with two different independent preparations of thylakoids from wild-type and ΔPsaJ plants could be modelled as the sum of three exponential decays as recently described in Zygadlo et al. (2005). From this it is clear that there is no significant difference in any of the estimated parameters suggesting that PsaJ in higher plants does not affect the electron transfer from PC to PSI. Thus, the explanation for the decrease in NADP+ photoreduction must be in the electron transport from P700 to Fd.

IV. Discussion

1. Role of APO1 in *psaA-psaB* translation, PSI accumulation and grana stacking

Regulation of PSI biogenesis and accumulation is important for establishing photosynthetic efficiency and the stoichiometric adjustment, for instance, if PSI-to-PSII ratios have to be balanced in response to exogenous or endogenous signals (Depège et al., 2003). Modulation of *psaA* and *psaB* gene expression at the levels of transcription (Allen and Pfannschmidt, 2000), transcript stability (Barkan and Goldschmidt-Clermont, 2000), translation (Zerges, 2000), and assembly of PSI (Schwabe and Kruip, 2000) represent key steps for such regulatory processes. APO1 is an indispensable component and plays a crucial role in the accumulation of the entire PSI complex and probably in photosystem adjustment *in vivo*. In higher plants the *psaA* and *psaB* genes are cotranscribed with *rps14* encoding subunit S14 of 30S plastid ribosomal moiety. We assume that translation of *rps14*, which is processed from the primary transcript (Lezhneva and Meurer, 2004), occurs independently and is functional in *apo1* because the general organelle translational machinery is intact in the mutant. The findings that ribosomal loading of *psaA-psaB* transcripts and, therefore, initiation of translation takes place in *apo1* and that liberation of *psaA-psaB* transcripts from ribosomes is retarded after lincomycin treatment in the mutant suggest that APO1 operates essentially at the level of translational elongation (Figure 6D). For example, when aconitase in prokaryotes and in the cytosol of eukaryotes loses its [4Fe-4S] cluster under iron starvation or oxidative stress, the altered iron regulatory protein binds specifically iron regulatory elements on mRNAs either to stabilize the transcripts or to block translation. How this specificity is achieved remains unknown (Kiley and Beinert, 2003), but it shows that reversible [4Fe-4S] cluster binding can be used to regulate translation. Synthesis or supply of chlorophyll and [4Fe-4S] clusters appears to play a crucial role in stabilization of PsaA and PsaB in chloroplasts (Mullet et al., 1990; Kim et al., 1994; Lezhneva et al., 2004). Because APO1 possesses Cys that could bind [4Fe-4S] clusters, it is reasonable to propose a possible role of APO1 in [4Fe-4S] cofactor assembly or cotranslational incorporation into PsaA and/or PsaB proteins. The function of APO1 could also be required for either still unknown steps in other pathways, like chlorophyll biosynthesis or incorporation of chlorophyll into PSI and antenna

proteins. This would explain the deficiency of LHC proteins and the loss of grana stacking in *apo1*.

2. Roles of APO1 in accumulation of other chloroplast [4Fe-4S] cluster–containing complexes

APO1 could have additional targets that interfere with chloroplast and/or thylakoid membrane development because several differences between *apo1* and other mutants specifically deficient in PSI became apparent. (1) The *apo1* mutant shows an albinotic phenotype when grown photoautotrophically. (2) The thylakoid membrane system is poorly developed and, surprisingly, lacks grana stacks but contains extended stroma-type lamellae. (3) The average size of the chloroplast is approximately 4 times smaller than in the wild-type or in other PSI mutants (Figure 7). (4) The impairment of the accumulation not only of the entire PSI complex but also of the outer PSI and PSII light-harvesting antennae as well as the absence of the corresponding fluorescence band at 77K are unique to *apo1* when compared with other PSI mutants (Figures 1 and 2; Lezhneva et al., 2004; Lezhneva and Meurer, 2004). (5) Members of the APO gene family are predicted to be localized in other cellular compartments like mitochondria. For *apo2* the protein was successfully imported into the chloroplast (data not shown); for *apo3* and *apo4* the same experiment showed no import into the organelle. It remains to be shown whether isoforms are imported into mitochondria. (6) Not only levels of PSI but also those of two other [4Fe-4S] cluster–containing protein complexes, FTR and NDH, are reduced in *apo1*. This suggests a specific role of APO1 in the accumulation of [4Fe-4S] cluster–containing complexes and could explain the pleiotropic phenotype.

Recently, a nuclear gene, Copper Response Defect1 (CRD1), which is responsible for PSI accumulation under copper starvation, was described from *Chlamydomonas* (Moseley et al., 2000, 2002). The *crd1* gene shows similarities to genes in photosynthetic organisms and has been suggested to be required for the synthesis of protochlorophyllide (Tottey et al., 2003). The failure of *apo1* to accumulate the core as well as the outer antenna of PSI is in common with the *crd1* mutant under copper starvation. However, the *Arabidopsis crd* antisense lines are predominantly affected in the levels of chlorophyll binding proteins but not in those of the photosynthetic core complexes (Tottey et al., 2003).

Therefore, the function of APO1 may be substantially different from that of CRD1. The *Chlamydomonas* mutants *tab1* and *tab2*, which are primarily affected in initiation of *psa*B translation, are also unable to translate the *psaA* mRNA as a result of a secondary effect of the mutation, designated the CES process (Stampacchia et al., 1997; Dauvillée et al., 2003; Wostrikoff et al., 2004). Provided that the CES process, which operates for plastid-encoded proteins, also occurs in higher plants, a failure to synthesize PsaA could be caused by the lack of *psaB* translation in *apo1*. Nonetheless, because levels of the nuclear-encoded FTR complex also are significantly reduced in *apo1*, it appears unlikely that APO1 is primarily involved in the CES process itself.

3. Comparison of the *apo1* and *hcf101* mutant phenotypes

Although HCF101 has been proposed to be involved in [4Fe-4S] cluster biogenesis, unlike *apo1*, the *hcf101* mutant is able

(1) to accumulate substantial amounts of the outer antenna proteins of PSI and PSII,

(2) to form grana stacks,

(3) to incorporate radiolabel into PsaA/B proteins *in vivo*, and

(4) to functionally load ribosomes with *psaA/psaB* transcripts (Lezhneva et al., 2004).

Ribosomal loading of *psaC*, however, is unaltered in *apo1* as well as in *hcf*101 mutants, although the PsaC protein contains two [4Fe-4S] clusters (Figure 3D; Lezhneva et al., 2004). Because of the stronger and pleiotropic phenotype of *apo1*, the function of the two proteins seems to be required for different though related pathways. For example, it is reasonable to assume that APO1 is essential for [4Fe-4S] (F_X) cofactor incorporation into PsaA and/or PsaB proteins during translation and, therefore, stabilization of the nascent peptide chains, whereas HCF101 could to be required for the incorporation of the [4Fe-4S] clusters F_A and F_B into the PsaC protein. Alternatively, APO1 could be involved in early stages of [4Fe-4S] cluster incorporation, and HCF101 could function in subsequent processes. On the other hand, the two factors could be required for diverse stages of the [4Fe-4S] cluster metabolism, like biogenesis, insertion, or stability. Similarly, it also remained uncertain at which step rubredoxin functions in [4Fe-4S] cluster metabolism during PSI assembly in cyanobacteria (Shen et al., 2002). In this context, it should be mentioned that HCF101 and APO1 are also

involved in the stable assembly of the nuclear-encoded, soluble FTR complex. It also remains to be shown at which stage during the assembly of the FTR the two factors are required.

4. Association of chloroplast gene expression to plastid nucleoids

Although it has been reported that initiation of both transcription and translation occurs in membrane-associated nucleoids of *Escherichia coli* (Simon and Nisman, 1977), little is known about the nucleoid organization, the interacting proteins, and processes leading to phase separation between nucleoids and the stroma or membranes in the chloroplast system (Herrmann et al., 1970; Kobayashi et al., 2002; Sato et al., 2003). In bacteria the specific association of ribosomes with nucleoids is a dynamic process including synthesis of RNA (Mascarenhas et al., 2001). The situation in the chloroplast may resemble the mitochondrial/eubacterial system, in which it has recently been shown that efficient expression of genes involves a complex series of interactions that localize transcriptionally active complexes in the nucleoids to the inner membrane surface to coordinate translational and transcriptional events (Rodeheffer and Shadel, 2003). There is increasing evidence that chloroplast gene expression occurs at the inner envelope membrane, and it has been shown that nucleoids are associated with the inner envelope membrane in differentiating chloroplasts (Kowallik et al., 1972; Sato et al., 1999; Zerges, 2000). These findings are relevant to the possible roles of APO1. The localization of APO1 close to the nucleoids suggests that translation of plastid-encoded genes and early PSI biogenesis are associated with the DNA-containing subplastidial compartment. It is feasible that initiation and the first steps of translation elongation take place in transcriptionally active nucleoids, but late translational events occur at different places, for example, in the matrix or in association with membranes. APO1 seems to be preferentially associated with transcriptionally and translationally active nucleoids, reflecting its higher affinity to individual nucleoids inside the chloroplast (Figure 9).

5. The novel APO repeat gene family contains four distinct groups in vascular plants

Remarkably, the APO1 start codon is localized in the second exon, indicating that the first exon is untranslated. APO1 is a member of a novel gene family with unknown function

encoding proteins consisting of 327 to 449 amino acid residues and exclusively found in vascular plants (Figure 10B). The size variation is mainly a result of different lengths of the N-terminal part in the individual groups APO1 to APO4 (Figure 10A). The APO gene family is characterized by a duplicated region of 100 amino acid residues (APO motifs 1 and 2) that is highly conserved among all members. These characteristics are indicative of a symmetric structure of APO proteins and probably of a symmetric ligand. On the other hand, APO1 could bind two similar ligands. Interestingly, four genes are present in *Arabidopsis*, and the corresponding orthologs were also found in rice (Figure 10B). The orthologs are similar in size and share the same sequence characteristics that are specific for each of the four APO groups. APO2 and APO3 in rice are computed to be localized in the chloroplast as well. Therefore, the function of APO1 could be partially redundant. The conservation of these four gene copies in vascular plants indicates that they have specific functions not only in the chloroplast but also in other cellular compartments.

Inactivation of the tobacco chloroplat *psaJ* gene

The successful generation of transplastomic *Nicotiana tabacum* plants devoid of the J subunit of PSI allowed for the first time to investigate the role of the PsaJ-subunit in higher plants. The PsaJ-less plants have been analysed by using various biochemical and physiological methods.

6. PsaJ is required for stable accumulation of PSI

In the absence of PsaJ the steady-state accumulation of PSI is reduced by 50% suggesting that PsaJ is required for stability or assembly of the PSI complex in tobacco. This contrasts results reported for *Chlamydomonas* lacking PsaJ, where it was concluded that steady-state accumulation of PSI does not require the PsaJ subunit (Fischer et al., 1999). Differences between higher plants and green algae with respect to PSI stability and function have also been reported after removal of subunit PsaF (Haldrup et al., 2000). In this study the absence of PsaF resulted in a severe destabilization of PSI and especially in a loss of the subunits at the stromal face like PsaC, -D and -E. In *Chlamydomonas* a deletion of PsaF did not affect the stability of the PSI complex (Farah et al., 1995; Fischer et al., 1999).

Transgenic *Arabidopsis* plants without PsaN, PsaH, PsaK and PsaL (Haldrup et al., 1999; Naver et al., 1999; Jensen et al., 2000, Lunde et al., 2003) compensate for a poorly functioning PSI by accumulating 18 - 20% more PSI. Apparently, the plants devoid of PsaJ cannot compensate in a similar way and this suggests that PsaJ affects the stability or assembly in a different way than the absence of PsaN, -H, -K or -L. Whether it is the stability or the assembly of the PSI complex that is affected remains to be solved.

The smaller amount of PSI was visible on the transgenic tobacco plants which were slightly smaller and paler when compared to wildtype. Plants devoid of the subunits PsaG or PsaK show also a decrease in size (Varotto et al., 2002); plants devoid of PsaG show a 40% reduction in PSI content (Jensen et al., 2002) and also a slightly lighter pigmentation (Varotto et al., 2002). Thus, there is a good correlation between the amount of PSI, leaf size and pigmentation.

7. PsaJ is required for efficient electron transport through PSI

PSI-J affects the electron transport through PSI: in the absence of the subunit J a 50 - 60 % decrease of the steady state electron transport, measured as $NADP^+$ *in vitro* photoreduction activity through PSI, is seen. The kinetic analysis of the PSI-PC interaction did not reveal any difference in any of the kinetic parameters between wild-type and the PsaJ deficient plants. Identical PC kinetics with PSI from ΔPsaJ and wildtype *Chlamydomonas* was also reported by Fischer et al. (1999) and it seems that PsaJ does not participate directly in the binding of PC both in plants and green algae. In contrast to the data obtained by Fischer et al. (1999) a decrease in the amplitude of the two fast components of electron transfer probably caused by an increased proportion of PSI complexes incompetent for fast electron transfer in the absence of PsaJ was not observed and therefore a stabilizing effect of PsaJ on PsaF is not very likely. Proper function of the donor side of PSI requires three low molecular mass subunits, namely PsaF, PsaN, and PsaJ. PsaF and PsaJ are membrane integral subunits. Their main functions are stabilization of the core antenna system and interaction with the peripheral antenna. In the case of PsaF there is also a well documented interaction with PC. PsaN is a luminal subunit which is involved in electron transport from PC (Haldrup et al., 1999).

The slower electron transport through PSI in the absence of PsaJ leads to a more reduced plastoquinone pool, this means an increased PSII excitation pressure, even under normal light conditions.

8. PSI-J is not necessary for binding of the peripheral light-harvesting antenna

The two chlorophylls bound to PsaJ in higher plants have been suggested to be important for the energy transfer between LHCI and the PSI core (Ben-Shem et al., 2003). The functional PSI antenna size is unaffected if PsaJ is removed from the PSI complex and binding of the various Lhca proteins to the PSI core is also unchanged. Thus, PsaJ is not required for binding of the peripheral antenna. However, the measurements of the functional antenna size using P700 oxidation rates do not possess sufficient time resolution to tell whether the absence the two chlorophyll molecules bound to PSI-J causes an inefficient transfer of excitation energy from the peripheral antenna to the core. Work with time resolved spectroscopy is in progress.

V. Summary

1. APO-project

The assembly of Fe-S clusters and their insertion into polypeptides has recently become an area of intense research. Plant cells can carry out both photosynthesis and respiration – two processes that require significant amounts of Fe-S proteins (Balk and Lobréaux, 2005). To investigate the nuclear-controlled mechanisms of [4Fe-4S] cluster assembly in chloroplasts, *Arabidopsis thaliana* mutants with a decreased content of photosystem I were selected. This photosystem contains three [4Fe-4S] clusters. One of the identified genes, ACCUMULATION OF PHOTOSYSTEM ONE (APO1), belongs to a previously unknown gene family with four defined members (APO1 to APO4) that are only found in nuclear genomes of vascular plants. All homologs contain two related motifs of approximately 100 amino acid residues that could potentially provide ligands for [4Fe-4S] clusters. APO1 is required for photoautotrophic growth, and levels of PSI core subunits are below the limit of detection in the *apo1* mutant. Unlike other *Arabidopsis* PSI mutants, *apo1* fails to accumulate significant amounts of the outer antenna subunits of PSI and PSII and to form grana stacks. In particular, APO1 is essential for stable accumulation of other plastid-encoded and nuclear-encoded [4Fe-4S] cluster complexes within the chloroplast, whereas [2Fe-2S] cluster-containing complexes appear to be unaffected. *In vivo* labeling experiments and analyses of polysome association suggest that translational elongation of the PSI transcripts *psa*A and/or *psa*B is arrested in the mutant. Taken together, our findings suggest that APO1 is involved in the stable assembly of several [4Fe-4S] cluster-containing complexes of chloroplasts and interferes with translational events probably in association with plastid nucleoids.

2. PsaJ-project

The plastid encoded gene *psaJ* encodes a hydrophobic low molecular mass subunit of photosystem I containing one transmembrane helix. The role of PSI-J was investigated in tobacco plants by inactivation of the *psaJ* gene. Homoplastomic transformants with an inactivated *psaJ* gene were able to grow photoautotrophically but were slightly smaller and paler than wild-type plants. The paler appearance is caused by an approximately 13% reduction in chlorophyll content per leaf area. This in mainly caused by an almost 50% reduction in PSI core proteins in plants devoid of PsaJ compared to wild type plants. There was no specific effect on the content of subunits located close to PsaJ such as PsaF or any other core subunit of PSI. However, the lower content of PSI suggests that PsaJ is important for stability or assembly of the PSI complex. In contrast to the core subunits, the peripheral Lhca antenna proteins were present in excess compared to core proteins. This was apparent both from a blueshift of the photosystem I fluorescence band at 77K and immunoblotting using specific Lhca antibodies. However, the functional size of the PSI antenna was not increased suggesting that the excess Lhca proteins is not bound to the core complexes in the mutant. The specific PSI activity measured as $NADP^+$ photoreduction *in vitro* revealed an almost 50% reduction in electron transport through PSI in the absence of PsaJ. This decreased electron transfer could not be attributed to changes in interaction with the luminal electron donor plastocyanin. Thus, PsaJ is an important subunit of PSI that affects both electron transport through the complex and stability or assembly of the PSI complex.

VI. Acknowledgements

VII. Literature

Abdallah, F., Salamini, F., Leister, D. (2000) A prediction of the size and evolutionary origin of the proteome of chloroplasts of Arabidopsis. Trends Plant Sci. 4, 141-2.

Allen, J.F. and Forsberg, J. (2001) Molecular recognition in thylakoid structure and function. Trends Plant Sci.6, 317-326.

Allen, J.F., and Pfannschmidt, T. (2000) Balancing the two photosystems: Photosynthetic electron transfer governs transcription of reaction centre genes in chloroplasts. Philos. Trans. R. Soc. Lond. B. Biol. Sci. 355, 1351–1359.

Allen, J.F. & Nilsson, A. (1997) Redox signalling and the structural basis of regulation of photosynthesis by protein phosphorylation. Physiol.Plant. 100, 863-868.

Adam, Z. (2000) Chloroplast proteases: possible regulators of gene expression? Biochimie 82, 647-654.

Adam, Z. and Ostersetzer, O. (2001) Degradation of unassembled and damaged thylakoid proteins. Biochem Soc Trans 29, 427-430.

Altschul, S.F., **Madden, T.L**., **Schaffer, A.A**., **Zhang, J**., **Zhang, Z**., **Miller, W**., **Lipman, D.J**. (1997) Gapped BLAST and PSI-BLAST: a new generation of protein database search programs. Nucleic Acids Res. 17, 3389-402.

Arabidopsis Genome Initiative (2000): Analysis of the genome sequence of the flowering plant *Arabidopsis thaliana*. Nature 408, 796-815.

Arnon, D.I. (1949) Copper enzymes in isolated chloroplasts. Polyphenoloxidase in *Beta vulgaris*. Plant Physiol. 24, 1–13.

Barber, J. and Nield, J. (2002) Organization of transmembrane helices in photosystem II: comparison of plants and cyanobacteria. Philos. Trans. R. Soc. Lond. B Biol. Sci. 357, 1329-1335.

Barkan, A., Miles, D., Taylor, W.C. (1986) Chloroplast gene expression in nuclear, photosynthetic mutants of maize. EMBO J. 7:1421-7.

Barkan, A., **Walker, M**., **Nolasco, M**., **Johnson, D**. (1994) A nuclear mutation in maize blocks the processing and translation of several chloroplast mRNAs and provides evidence for the differential translation of alternative mRNA forms. EMBO J. 13, 3170-81.

Barkan, A. (1998) Approaches to investigating nuclear genes that function in chloroplast biogenesis in land plants. Methods Enzymol. 297, 38–57.

Barkan, A., and Goldschmidt-Clermont, M. (2000) Participation of nuclear genes in chloroplast gene expression. Biochimie 82, 559–572.

Beinert, H., Holm, R.H., and Munck, E. (2000) Iron-sulfur clusters: Nature's modular, multipurpose structures. Science 277, 653–659.

Ben-Shem, A., Frolow, F., and Nelson, N. (2003) Crystal structure of plant photosystem I. Nature 426, 630–635.

Bethesda Research Laboratories (1986) BRL pUC host: *E.coli* DH5a competent cells. Bethesda Res. Lab. Focus 8**,** pp 9-9.

Birnboim H.C. u. Doly J. (1979) A rapid alkaline extraction procedure for screening recombinant plasmid DNA. Nucl. Acids Res. 7, 1513-1523.

Blum, H., Beier, H., Gross, H. J. (1987) Improved silver staining of plant-proteins, RNA and DNA in polyacrylamide gels. Electrophoresis, 8, 93-99.

Bottin, H., Mathis, P. (1985) Interaction of plastocyanin with the photosystem I reaction center: a kinetic study by flash absorption spectroscopy, Biochemistry 24, 6453-6460.

Bruick, R.K., and Mayfield, S.P. (1999) Light-activated translation of chloroplast mRNAs. Trends Plant Sci. 4, 190–195.

Chitnis, P.R. (2001) Photosystem I: Function and physiology. Annu. Rev. Plant Physiol. Plant Mol. Biol. 52, 539–626.

Choquet, Y., and Wollman, F.A. (2002) Translational regulations as specific traits of chloroplast gene expression. FEBS Lett. 529, 39–42.

Clark RD, Hind G. (1983) Isolation of a five-polypeptide cytochrome b-f complex from spinach chloroplasts. J Biol Chem. 258:10348-54.

Clough, S.J., and Bent, A.F. (1998) Floral dip: A simplified method for Agrobacterium-mediated transformation of Arabidopsis thaliana. Plant J. 16, 735–743.

Cohen, A., Yohn, C.B., and Mayfield, S. (2001) Translation of the chloroplast-encoded psbD is arrested post-initiation in a nuclear mutant of Chlamydomonas reinhardtii. J. Plant. Physiol. 158, 1069–1075.

Danielsson, R., Albertsson, P., Mamedov, F. and Styring, S. (2004) Quantification, of photosystem I and II in different parts of the thylakoid membrane from Spinach. Biochimica et biophysica acta-ioenergetics 1608, 53-61.

Dauville´ e, D., Stampacchia, O., Girard-Bascou, J., and Rochaix, J.D. (2003) Tab2 is a novel conserved RNA binding protein required for translation of the chloroplast psaB mRNA. EMBO J. 22, 6378–6388.

Depège, N., Bellafiore, S., and Rochaix, J.D. (2003) Role of chloroplast protein kinase Stt7 in LHCII phosphorylation and state transition in Chlamydomonas. Science 299, 1572–1575.

Drepper, F., Hippler, M., Nitschke, W., Haehnel, W. (1996) Binding dynamics and electron transfer between plastocyanin and photosystem I. Biochemistry 35, 1282-1295.

Eichacker, L.A., Soll, J., Lauterbach, P., Rüdiger, W., Klein, R.R., and Mullet, J.E. (1990) In vitro synthesis of chlorophyll a in the dark triggers accumulation of chlorophyll a apoproteins in barley etioplasts. J. Biol. Chem. 265, 13566–13571.

Emanuelsson, O., **Nielsen, H.**, **von Heijne, G**. (1999) ChloroP, a neural network-based method for predicting chloroplast transit peptides and their cleavage sites. Protein Sci. 5, 978-84.

Evron, Y., Johnson, E.A., McCarty, R.E. (2000) Regulation of proton flow and ATP synthesis in chloroplasts. J Bioenerg Biomembr. 5:501-6.

Farah, J., Rappaport, F., Choquet, Y., Joliot, P. and Rochaix, J-D. (1995) Isolation of a psaF-deficient mutant of Chlamydomonas reinhardtii: efficient interaction of plastocyanin with the photosystem I reaction center is mediated by the PsaF subunit. EMBO J 14, 4976-4984.

Fedoroff, N.V. (2002) RNA-binding proteins in plants: The tip of an iceberg? Curr. Opin. Plant Biol. 5, 452–459.

Feinberg, A.P. and Vogelstein, B. (1983) A technique for radiolabeling DNA restriction endonuclease fragments to high specific activity. Anal Biochem. 132, 6-13.

Feldmann, K.A. (1991) T-DNA insertion mutagenesis in Arabidopsis: Mutational spectrum. Plant J. 1, 71–82.

Fischer N., Boudreau E., Hippler M., Drepper F., Haehnel, W. and Rochaix, J-D. (1999) A large fraction of PsaF is nonfunctional in photosystem I complexes lacking the PsaJ subunit. Biochemistry 38, 5546-5552.

Frazzon, J., and Dean, D.R. (2003) Formation of iron-sulfur clusters in bacteria: An emerging field in bioinorganic chemistry. Curr. Opin. Chem. Biol. 7, 166–173.

Frohman, M.A., Dush, M.K., and Martin, G.R. (1988) Rapid production of full-length cDNAs from rare transcripts: Amplification using a single gene-specific oligonucleotide primer. Proc. Natl. Acad. Sci. USA 85, 8998–9002.

Fromme, P., Jordan, P. and Krauss, N. (2001) Structure of photosystem I. Biochim Biophys Acta 1507, 5-31.

Ganeteg, U. (2004) Phd Thesis: The light-harvesting antenna of higher plant photosystem I (Umeå, Univ.).

Ganeteg, U., Klimmek, F. and Jansson, S. (2004) Lhca5 - an LHC-Type Protein Associated with Photosystem I. Plant Mol Biol 54, 641-651.

Golbeck, J.H. (2003) The binding of cofactors to photosystem I analyzed by spectroscopic and mutagenic methods. Annu. Rev. Biophys. Biomol. Struct. 32, 237–256.

Golbeck, J.H. (1992) Structure and function of photosystem I. Annu Rev Plant Physiol Plant Mol Biol 43: 293-324.

Goldschmidt-Clermont, M. (1998) Coordination of nuclear and chloroplast gene expression in plant cells. Int. Rev. Cytol. 177, 115–180.

Groth, G. and Pohl, E. (2001) The structure of the chloroplast F_1-ATPase at 3.2 Å resolution. J. Biol. Chem. 276, 1345–1352.

Groth, G. and Strotmann, H. (1999) New results about structure, function and regulation of the chloroplast ATP synthase (CF_0CF_1). Physiol. Plant. 106, 142-148.

Gruissem, W. (1989) Chloroplast gene expression: how plants turn their plastids on. Cell, 56, 161-170.

Grüne, H. and Westhoff, P. (1988) Transfer von RNA auf Pall Biodyne A Nylonmembranen und Immobilisierung mittels UV-Crosslinking. Pall BioSupport SD 1217 G.

Guruprasad, K., Reddy, B.V., and Pandit, M.W. (1990) Correlation between stability of a protein and its dipeptide composition: A novel approach for predicting in vivo stability of a protein from its primary sequence. Protein Eng. 4, 155–161.

Haldrup, A., Simpson , J.D. and Scheller, H.V. (2000) Down-regulation of the PSI-F subunit of Photosystem I in Arabidopsis thaliana. The PSI-F subunit is essential for photoautotrophic growth and antenna function. J Biol Chem 275, 31211-31218.

Haldrup, A., Naver, H., and Scheller, H. V. (1999) The interaction between plastocyanin and photosystem I is inefficient in transgenic Arabidopsis plants lacking the PSI-N subunit of photosystem I. Plant J. 17, 689–698.

Hanahan, D. (1983) Studies on transformation of Escherichia coli with plasmids. J Mol Biol. 4, 557-80.

Hankamer, B., Barber, J. and Boekema, E.J. (1997) Structure and membrane organisation of photosystem II in green plants. Annu. Rev. Plant Physiol. Plant Mol. Biol. 48, 641-671.

Hankamer, B., Morris, E., Nield, J., Carne, A. and Barber, J. (2001) Subunit positioning and transmembrane helix organization in the core dimer of photosystem II. FEBS Lett. 504, 142-151.

Havaux, M., and Niyogi, K.K. (1999) The violaxanthin cycle protects plants from photooxidative damage by more than one mechanism. Proc. Natl. Acad. Sci. USA 96, 8762–8767.

Herrmann, R.G., Kowallik, K.V. (1970) Selective presentation of DNA-regions and membranes in chloroplasts and mitochondria.J Cell Biol. 45:198-202.

Hippler, M., Rimbault, B. and Takahashi, Y. (2002) Photosynthetic complex assembly in *Chlamydomonas reinhardtii*. Protist 153, 197-220.

Hippler, M., Drepper, F., Haehnel, W. and Rochaix, J-D. (1998) The N-terminal domain of PsaF: Precise recognition site for binding and fast electron transfer from cytochrome c(6) and plastocyanin to photosystem I of Chlamydomonas reinhardtii. Proc Natl Acad Sci USA 95, 7339-7344.

Hippler, M., Drepper, F., Farah, J. and Rochaix, J-D. (1997) Fast electron transfer from cytochrome c(6) and plastocyanin to photosystem I of Chlamydomonas reinhardtii requires PsaF. Biochemistry 36, 6343-6349.

Hippler, M., Reichert, J., Sutter, M., Zak, E., Altschmied, L., Schroer, U., Herrmann, R.G., Haehnel, W. (1996) The plastocyanin binding domain of photosystem I. EMBO J. 15:6374-84.

Inoue, H., Tsuchiya, T., Satoh, S., Miyashita, H., Kaneko, T., Tabata, S., Tanaka, A., Mimuro, M. (2004) Unique constitution of photosystem I with a novel subunit in the cyanobacterium Gloeobacter violaceus PCC 7421. FEBS Lett. 578, 275-9.

Jansson, S., Stefansson, H., Nystrom, U., Gustafsson, P. and Albertsson, P.-A. (1997) Antenna protein composition of PS I and PS II in thylakoid sub-domains. Biochimica et Biophysica Acta (BBA) - Bioenergetics 1320, 297-309.

Jansson, S., Andersen, B., and Scheller, H.V. (1996) Nearest neighbor analysis of higher-plant photosystem I holocomplex. Plant Physiol 12: 409-420.

Jenkins, B.D., **Kulhanek, D.J**., **Barkan, A**. (1997) Nuclear mutations that block group II RNA splicing in maize chloroplasts reveal several intron classes with distinct requirements for splicing factors. Plant Cell. 3, 283-96.

Jensen, P. E., Haldrup, A., Zhang, S. and Scheller, H. V. (2004) The PSI-O subunit of plant photosystem I is involved in balancing the excitation pressure between the two photosystems. J Biol Chem 279, 24212-24217.

Jensen, P. E., Haldrup, A., Rosgaard, L. and Scheller, H. V. (2003) Molecular dissection of photosystem I in higher plants: topology, structure and function. Physiol Plant 119, 313-321.

Jensen, P. E., Gilpin, M., Knoetzel, J., and Scheller, H. V. (2000) The PSI-K subunit of photosystem I is involved in the interaction between light-harvesting complex I and the photosystem I reaction center core. J. Biol. Chem. 275, 24701–24708.

Jordan, P., Fromme, P., Witt, H.T., Klukas, O., Saenger, W., and Krauss, N. (2001) Three-dimensional structure of cyanobacterial photosystem I at 2.5 Å resolution. Nature 411, 909–917.

Kiley, P.J., and Beinert, H. (2003) The role of Fe-S proteins in sensing and regulation in bacteria. Curr. Opin. Microbiol. 6, 181–185.

Kim, J., Eichacker, L.A., Rüdiger, W., and Mullet, J.E. (1994) Chlorophyll regulates accumulation of the plastid-encoded chlorophyll proteins P700 and D1 by increasing apoprotein stability. Plant Physiol. 104, 907–916.

Klimmek, F., Ganeteg, U., Ihalainen, J.A., van Roon, H., Jensen, P.E., Dekker, J.P., Scheller, H.V. & Jansson, S. (2005) The structure of higher plant LHCI − in vivo characterization and structural interdependence of the Lhca proteins. *Biochemistry* 44, 3065-3073.

Klughammer, C. and Schreiber, U. (1998) Measuring P700 absorbance changes in the near infrared spectral region with a dual wavelength pulse modulation system, in: Garab G. (ed), Photosynthesis: Mechanisms and Effects, vol. V, Kluwer Academic Publishers, Dordrecht, pp. 4357-4360.

Klughammer, C., and Schreiber, U. (1994) An improved method, using saturating light pulses, for the determination of photosystem I quantum yield via P700þ-absorbance changes at 830 nm. Planta 192, 261–268.

Kamiya, N. and Shen, J.R. (2003) Crystal structure of oxygenevolving photosystem II from *Thermosynechococcus vulcanus* at 3.7 Å resolution. Proc. Natl. Acad. Sci. USA 100, 98-103.

Kashino, Y., Lauber, W.M., Carroll, J.A., Wang, Q., Whitmarsh, J., Satoh, K. and Pakrasi, H.B. (2002) Proteomic analysis of a highly active photosystem II preparation from the cyanobacterium *Synechocystis* sp. PCC 6803 reveals the presence of novel polypeptides. Biochemistry 41, 8004-8012.

Kobayashi, T., Takahara, M., Miyagishima, S.Y., Kuroiwa, H., Sasaki, N., Ohta, N., Matsuzaki, M., and Kuroiwa, T. (2002) Detection and localization of a chloroplast-encoded HU-like protein that organizes chloroplast nucleoids. Plant Cell 14, 1579–1589.

Koncz C, Nemeth K, Redei GP, Schell J. (1992) T-DNA insertional mutagenesis in Arabidopsis. Plant Mol Biol. 5, 963-76.

Kowallik, K.V., **Herrmann, R.G.** (1972) Variable amounts of DNA related to the size of chloroplasts. IV. Three-dimensional arrangement of DNA in fully differentiated chloroplasts of Beta vulgaris L. J Cell Sci. 11:357-77.

Krause, G.H., and Weis, E. (1991) Chlorophyll fluorescence and photosynthesis: The basics. Annu. Rev. Plant. Physiol. Plant Mol. Biol. 42, 313–349.

Kubicki, A., Funk, E., Westhoff, P., Steinmüller, K. (1996) Differential expression of plastome-encoded *ndh*-genes in the mesophyll and bundle-sheat chloroplasts of the C4-plant *Sorhum bicolour* indicates that the complex I-homologous NAD(P)H-plastoquinone-oxireductase is involved in cyclic electron transport. Planta 199, 276-281.

Kurisu, G., Zhang, H., Smith, J.L. and Cramer, W.A. (2003) Structure of the cytochrome b_6f complex of oxygenic photosynthesis: tuning the cavity. Science 302, 1009-1014.

Legen, J., Misera, S., Herrmann, R.G., and Meurer, J. (2001) Map positions of 69 Arabidopsis thaliana genes of all known nuclear encoded constituent polypeptides and various regulatory factors of the photosynthetic membrane: A case study. DNA Res. 27, 53–60.

Leister, D. and Schneider, A. (2003) From genes to photosynthesis in *Arabidopsis thaliana*. Int Rev Cytol 228, 31-83.

Leon, P., Arroyo, A., and Mackenzie, S. (1998) Nuclear control of plastid and mitochondrial development in higher plants. Annu. Rev. Plant Physiol. Plant Mol. Biol. 49, 453–480.

Léon, S., Touraine, B., Ribot, C., Briat, J.F., and Lobréaux, S. (2003) Iron-sulphur cluster assembly in plants: Distinct NFU proteins in mitochondria and plastids from Arabidopsis thaliana. Biochem. J. 371, 823–830.

Levy, H., **Kindle, K.L**., **Stern, D.B**. (1997) A Nuclear Mutation That Affects the 3[prime] Processing of Several mRNAs in Chlamydomonas Chloroplasts. Plant Cell. 5, 825-836.

Levy, H., **Kindle, K.L**., **Stern, D.B**. (1999) Target and specificity of a nuclear gene product that participates in mRNA 3'-end formation in Chlamydomonas chloroplasts.J Biol Chem. 50, 35955-62.

Lezhneva, L., Amann, K., and Meurer, J. (2004) The universally conserved HCF101 protein is involved in assembly of [4Fe-4S]-cluster containing complexes in Arabidopsis thaliana chloroplasts. Plant J. 37, 174–185.

Lezhneva, L., and Meurer, J. (2004) The nuclear factor HCF145 affects chloroplast psaA-psaBrps14 transcript abundance in Arabidopsis thaliana. Plant J. 38, 740–753.

Lichtenthaler, H. K. (1987) Chlorophylls and carotenoids – pigments of photosynthetic bio-membranes. Methods Enzymol. 148, 350–382.

Lill, R., and Kispal, G. (2000) Maturation of cellular Fe-S proteins: An essential function of mitochondria. Trends Biochem. Sci. 25, 352–356.

Liu, Z., Yan, H., Wang, K., Kuang, T., Zhang, J., Gui, L., An, X. and Chang, W. (2004) Crystal structure of spinach major light-harvesting complex at 2.72 Å resolution. Nature 428, 287-292.

Lizardi, P.M. (1983) Methods for the preparation of messenger RNA. Meth. Enzymol. 96, 24-38.

Lunde, C., Jensen, P. E., Rosgaard, L., Haldrup, A., Gilpin, M. J., and Scheller, H. V. (2003) Plant Cell Physiol. 44, 44–54.

Lunde, C., Jensen, P. E., Haldrup, A., Knoetzel, J., and Scheller, H. V. (2000) The PSI-H subunit of photosystem I is essential for state transitions in plant photosynthesis. Nature 408, 613–615.

Lyznik, L.A., Peng, J.Y., and Hodges, T.K. (1991) Simplified procedure for transient transformation of plant protoplasts using polyethylene glycol treatment. Biotechniques 10, 294–300.

Martin W, Herrmann RG. (1998) Gene transfer from organelles to the nucleus: how much, what happens, and Why? Plant Physiol. 118, 9-17.

Martin, W. (2003) Gene transfer from organelles to the nucleus: frequent and in big chunks. Proc Natl Acad Sci U S A. 5:8612-4.

Mascarenhas, J., Weber, M.H., and Graumann, P.L. (2001) Specific polar localization of ribosomes in Bacillus subtilis depends on active transcription. EMBO Rep. 2, 685–689.

McCormac, D.J., and Barkan, A. (1999) A nuclear gene in maize required for the translation of the chloroplast atpB/E mRNA. Plant Cell 11, 1709–1716.

McMaster GK, **Carmichael GG.** (1997) Analysis of single- and double-stranded nucleic acids on polyacrylamide and agarose gels by using glyoxal and acridine orange. Proc Natl Acad Sci U S A. 11, 4835-8.

Merchant, S., and Dreyfuss, B.W. (1998) Posttranslational assembly of photosynthetic metalloproteins. Annu. Rev. Plant Physiol. Plant Mol. Biol. 49, 25–51.

Meurer, J., Lezhneva, L., Amann, K., Gödel, M., Bezhani, S., Sherameti, I., Oelmuller, R. (2002) A peptide chain release factor 2 affects the stability of UGA-containing transcripts in Arabidopsis chloroplasts. Plant Cell. 12:3255-69.

Meurer, J., Berger, A., and Westhoff, P. (1996b) A nuclear mutant of Arabidopsis with impaired stability on distinct transcripts of the plastid psbB, psbD/C, ndhH, and ndhC operons. Plant Cell 8, 1193–1207.

Meurer, J., Grevelding, C., Westhoff, P., and Reiss, B. (1998a) The PAC protein affects the maturation of specific chloroplast mRNAs in Arabidopsis thaliana. Mol. Gen. Genet. 258, 342–351.

Meurer, J., Meierhoff, K., and Westhoff, P. (1996a) Isolation of highchlorophyll-fluorescence mutants of Arabidopsis thaliana and their characterization by spectroscopy, immunoblotting and Northern hybridization. Planta 198, 385–396.

Meurer, J., Plücken, H., Kowallik, K.V., and Westhoff, P. (1998b) A nuclear-encoded protein of prokaryotic origin is essential for the stability of photosystem II in Arabidopsis thaliana. EMBO J. 17, 5286–5297.

Mollier, P., Hoffmann, B., Debast, C., and Small, I. (2002) The gene encoding Arabidopsis thaliana mitochondrial ribosomal protein S13 is a recent duplication of the gene encoding plastid S13. Curr. Genet. 40, 405–409.

Moseley, J.L., Page, M.D., Alder, N.P., Eriksson, M., Quinn, J., Soto, F., Theg, S.M., Hippler, M., and Merchant, S. (2002) Reciprocal expression of two candidate di-iron enzymes affecting photosystem I and light-harvesting complex accumulation. Plant Cell 14, 673–688.

Moseley, J.L., Quinn, J., and Merchant, S. (2000) The Crd1 gene encodes a putative di-iron enzyme required for photosystem I accumulation in copper deficiency and hypoxia in Chlamydomonas reinhardtii. EMBO J. 19, 2139–2151.

Mullet, J.E., Klein, P.G., and Klein, R.R. (1990) Chlorophyll regulates accumulation of the plastid-encoded chlorophyll apoproteins CP43 and D1 by increasing apoprotein stability. Proc. Natl. Acad. Sci. USA 87, 4038–4042.

Munekage, Y., Hojo, M., Meurer, J., Endo, T., Tasaka, M., and Shikanai, T. (2002) PGR5 is involved in cyclic electron flow around photosystem I and is essential for photoprotection in Arabidopsis. Cell 110, 361–371.

Murashige, T. and Skoog, F. (1962) A revised medium for rapid growth and bio assays with tobacco tissue cultures. Physiol.Plant. 15, 473-497.

Nakamura, Y., Kaneko, T., Sato, S., Mimuro, M., Miyashita, H., Tsuchiya, T., Sasamoto, S., Watanabe, A., Kawashima, K., Kishida, Y., Kiyokawa, C., Kohara, M., Matsumoto, M., Matsuno, A., Nakazaki, N., Shimpo, S., Takeuchi, C., Yamada, M., Tabata, S. (2003) Complete genome structure of Gloeobacter violaceus PCC 7421, a cyanobacterium that lacks thylakoids. DNA Res. 10, 137-45.

Naver, H., Haldrup, A., and Scheller, H.V. (1999) Cosuppression of photosystem I subunit PSI-H in Arabidopsis thaliana. Efficient electron transfer and stability of photosystem I is dependent upon the PSI-H subunit.J.Biol.Chem.274, 10784-10789.

Naver, H., Scott, M.P., Golbeck, J.H., Møller, B.L. and Scheller, H.V. (1996) Reconstitution of barley photosystem I with modified PSI-C allows identification of domains interacting with PSI-D and PSI-A/B. J. Biol. Chem. 271, 8996-9001.

Nickelsen, J. (2003) Chloroplast RNA-binding proteins. Curr Genet 43, 392-399.

Nordling, M., Sigfridsson, K., Young, S., Lundberg, L.G., Hansson, Ö. (1991) Flash-photolysis studies of the electron transfer from genetically modified spinach plastocyanin to photosystem I, FEBS Lett. 291, 327-330.

Pilon-Smits, E.A., Garifullina, G.F., Abdel-Ghany, S., Kato, S., Mihara, H., Hale, K.L., Burkhead, J.L., Esaki, N., Kurihara, T., and Pilon, M. (2002) Characterization of a NifS-like chloroplast protein from Arabidopsis. Implications for its role in sulfur and selenium metabolism. Plant Physiol. 130, 1309–1318.

Radford, M.M. (1976) A rapid and sensitive method for the quantitation of microgram quantities of protein utilizing the principle of protein-dye binding. Anal Biochem. 72, 248-54.

Rattanachaikunsopon, P., Rosch, C., and Kuchka, M.R. (1999) Cloning and characterization of the nuclear AC115 gene of Chlamydomonas reinhardtii. Plant Mol. Biol. 9, 1–10.

Rhee, K.H. (2001) Photosystem II: the solid structural era. Annu. Rev. Biophys. Biomol. Struct. 30, 307-328.

Rochaix JD, Perron K, Dauvillee D, Laroche F, Takahashi Y, Goldschmidt-Clermont (2004) Post-transcriptional steps involved in the assembly of photosystem I in Chlamydomonas. Biochem Soc Trans. 32, 567-70.

Rodeheffer, M.S., and Shadel, G.S. (2003) Multiple interactions involving the amino-terminal domain of yeast mtRNA polymerase determine the efficiency of mitochondrial protein synthesis. J. Biol. Chem. 278, 18695–18701.

Rodermel, S. (2001) Pathways of plastid-to-nucleus signaling. Trends Plant Sci 6, 471-478.

Saenger, W., Jordan, P., Krauss, N. (2002) The assembly of protein subunits and cofactors in photosystem I.Curr Opin Struct Biol. 12, 244-54.

Sambrook J., Fritsch E.F. u. Maniatis T. (1989) Molecular cloning: A Laboratory Manual, 2nd edition. Cold Spring Harbor Laboratory Press. Cold Spring Harbor, New York.

Sato, N., Terasawa, K., Miyajima, K., and Kabeya, Y. (2003) Organization, developmental dynamics, and evolution of plastid nucleoids. Int. Rev. Cytol. 232, 217–262.

Sato, S., Nakamura, Y., Kaneko, T., Asamizu, E., and Tabata, S. (1999) Complete structure of the chloroplast genome of Arabidopsis thaliana. DNA Res. 6, 283–290.

Scheller, H.V., Jensen, P.E., Haldrup, A., Lunde, C., and Knoetzel, J. (2001) Role of subunits in eukaryotic Photosystem I. Biochim. Biophys. Acta 1507, 41–60.

Schöneberg, U., Vahrson, W., Priedemuth, U. und Wittig, B. (1993) Analysis and Interpretation of DNA and Protein Sequences Using MacMolly Tetra®. Bielefeld, KAROI-Verlag.

Schwabe, T.M., and Kruip, J. (2000): Biogenesis and assembly of photosystem I. Indian J. Biochem. Biophys. 37, 351–359.

Shen, G., Antonkine, M.L., van der Est, A., Vassiliev, I.R., Brettel, K., Bittl, R., Zech, S.G., Zhao, J., Stehlik, D., Bryant, D.A., and Golbeck, J.H. (2002) Assembly of photosystem I. II. Rubredoxin is required for the in vivo assembly of F(X) in Synechococcus sp. PCC 7002 as shown by optical and EPR spectroscopy. J. Biol. Chem. 277, 20355–20366.

Sigfridsson, K., Young, S., Hansson, Ö. (1996) Structural dynamics in the plastocyanin-photosystem 1 electron-transfer complex as revealed by mutant studies, Biochemistry 35, 1249-1257.

Simon, M.C., and Nisman, B. (1977): Initiation of transcription and translation in E. coli nucleoids. C. R. Acad. Sci. Hebd. Seances Acad. Sci. D. 285, 435–438.

Sommer, F., Drepper, F., Hippler, M. (2002) The luminal helix l of PsaB is essential for recognition of plastocyanin or cytochrome c(6) and fast electron transfer to photosystem I in Chlamydomonas reinhardtii. J Biol Chem 277, 6573-6581.

Stampacchia, O., Girard-Bascou, J., Zanasco, J.L., Zerges, W., Bennoun, P., and Rochaix, J.D. (1997) A nuclear-encoded function essential for translation of the chloroplast psaB mRNA in Chlamydomonas. Plant Cell 9, 773–782.

Stern, D.B., Higgs, D.C., and Yang, J. (1997) Transcription and translation in chloroplasts. Trends Plant Sci. 2, 308–315.

Sticht, H., and Rösch, P. (1998) The structure of iron-sulfur proteins. Prog. Biophys. Mol. Biol. 70, 95–136.

Stroebel D, Choquet Y, Popot JL, Picot D. (2003) An atypical haem in the cytochrome b(6)f complex. Nature 426, 413-8.

Strotmann, H., Shavit, N. and Leu, S. (1998) Assembly and function of the chloroplast ATP synthase. In: The molecular biology of chloroplast and mitochondria in *Chlamydomonas* (Rochaix, J.D., Goldschmidt-Clermont, M. and Merchant, S., eds). Norwell, MA: Kluwer Academic Publishers, pp. 477–500.

Sugiura, M., Hirose, T., and Sugita, M. (1998) Evolution and mechanism of translation in chloroplasts. Annu. Rev. Genet. 32, 437–459.

Surpin, M., Larkin, R.M., and Chory, J. (2002) Signal transduction between the chloroplast and the nucleus. Plant Cell 14, 327–338.

Svab, Z., Maliga, P. (1993) High-frequency plastid transformation in tobacco by selection for a chimeric aadA gene. Proc Natl Acad Sci U S A. 90, 913-7.

Swiatek, M., Greiner, S., Kemp, S., Drescher, A., Koop, H.U., Herrmann, R.G., Maier, R.M. (2003) PCR analysis of pulsed-field gel electrophoresis-purified plastid DNA, a sensitive tool to judge the hetero-/homoplastomic status of plastid transformants. Curr Genet. 43, 45-53.

Tottey, S., Block, M.A., Allen, M., Westergren, T., Albrieux, C., Scheller, H.V., Merchant, S., and Jensen, P.E. (2003) Arabidopsis CHL27, located in both envelope and thylakoid membranes, is required for the synthesis of protochlorophyllide. Proc. Natl. Acad. Sci. USA 100, 16119–16124.

Touraine, B., Boutin, J.-P., Marion-Poll, A., Briat, J.-F., Peltier, G., and Lobréaux, S. (2004) Nfu2: A scaffold protein required for [4Fe-4S] and ferredoxin iron-sulphur cluster assembly in Arabidopsis chloroplasts. Plant J. 40, 101–111.

Varotto, C., Pesaresi, P., Jahns, P., Lessnick, A., Tizzano, M., Schiavon, F., Salamini, F. and Leister, D. (2002) Single and double knockouts of the genes for photosystem I subunits G, K, and H of *Arabidopsis*. Effects on photosystem I composition, photosynthetic electron flow, and state transitions. Plant Physiol. 129, 616-624.

Vogel, J., Borner, T. and Hess, W. R. (1999) Comparative analysis of splicing of the complete set of chloroplast group II introns in three higher plant mutants. Nucleic Acids Res 27, 3866-3874.

Wittwer, C.T., Ririe, K.M., Andrew, R.V., David, D.A., Gundry, R.A., and Balis, U.J. (1997) The LightCycler: A microvolume multisample fluorimeter with rapid temperature control. Biotechniques 22, 176–181.

Westhoff, P. and Hermann, R.G. (1988) Complex RNA maturation in chloroplasts: The *psbB* operon from spinach. Eur. J. Biochem. 171, 551-564.

Westhoff, P., Offermann-Steinhard, K., Höfer, M., Eskins, K., Oswald, A., and Streubel, M. (1991) Differential accumulation of plastid transcripts encoding photosystem II components in the mesophyll and bumdle-sheat cells of monocotyledonous NADP-malic enzyme-type C4 plants. Planta 184, 377-388

Wollman, F. A., Minai, L. and Nechushtai, R. (1999) The biogenesis and assembly of photosynthetic proteins in thylakoid membranes1. Biochim Biophys Acta 1411, 21-85.

Wostrikoff, K., Girard-Bascou, J., Wollman, F.A., and Choquet, Y. (2004) Biogenesis of PSI involves a cascade of translational autoregulation in the chloroplast of Chlamydomonas. EMBO J. 23, 2696–2705.

Xu, Q., Yu, L., Chitnis, V.P. and Chitnis, P.R. (1994a) Function and organization of photosystem I in a cyanobacterial mutant strain that lacks PsaF and PsaJ subunits. J Biol Chem 269, 3205-3211.

Xu, W., Jung, Y.S., Chitnis, V.P., Guikema, J.A., Golbeck, J.H. and Chitnis, P.R. (1994b) Mutational analysis of photosystem I polypeptides in the cyanobacterium Synechocystis sp. PCC 6803. J Biol Chem 269, 21512-21518.

Yabe, T., Morimoto, K., Kikuchi, S., Nishio, K., Terashima, I., and Nakai, M. (2004) The Arabidopsis chloroplastic NifU-like protein CnfU, which can act as an iron-sulfur cluster scaffold protein, is required for biogenesis of ferredoxin and photosystem I. Plant Cell 16, 993–1007.

Yu, J., Vassiliev, I. R., Jung, Y. S., Golbeck, J. H. and McIntosh, L. (1997) Strains of *Synecho cystis* sp. PCC 6803 with altered PsaC. I. Mutations incorporated in the cysteine ligands of the two [4Fe-4S] clusters FA and FB of photosystem I. J Biol Chem 272, 8032-8039.

Zerges, W. (2000) Translation in chloroplasts. Biochimie 82, 583–601.

Zhang, S. and Scheller, H.V. (2004) Light-harvesting complex II binds to several small subunits of photosystem I. J. Biol. Chem. 279, 3180-3187.

Zygadlo, A., Jensen, P.E., Leister, D. and Scheller, H.V. (2005) Photosystem I lacking the PSI-G subunit has higher affinity for plastocyanin and is less stable. Biochim. Biophys. Acta. to photodamage.1708:154-63.

List of publications

Parts of this work have already been published or are in preparation to be published:

Amann, K., Lezhneva, L., Wanner, G., Herrmann, R.G. and Meurer J. (2004) ACCUMULATION OF PHOTOSYSTEM ONE1, a member of a novel gene family, is required for accumulation of [4Fe-4S] cluster-containing chloroplast complexes and antenna proteins. Plant Cell 16, 3084-3097

Katrin Amann, Andreas Hansson, Agnieszka Zygadlo, Jörg Meurer, Henrik Vibe Scheller and Poul Erik Jensen Knock-out of the PSI-J Subunit of Photosystem I (PSI) in *Nicotiana tabacum:* PSI-J is required for efficient electron transport and stability of the multiprotein complex.

Lezhneva, L., Amann, K., and Meurer, J. (2004) The universally conserved HCF101 protein is involved in assembly of [4Fe-4S]-cluster containing complexes in Arabidopsis thaliana chloroplasts. Plant J. 37, 174–185

Meurer, J., Lezhneva, L., Amann, K., Gödel, M., Bezhani, S., Sherameti, I. and Oelmüller, R. (2002) A peptide chain release factor 2 affects the stability of UGA-containing transcripts in Arabidopsis chloroplasts. Plant Cell 14, 3255-3269

Ehrenwörtliche Versicherung

Hiermit versichere ich, daß ich die vorliegende Arbeit selbständig und nur unter Verwendung der angegebenen Hilfsmittel und Quellen angefertigt habe.
Zudem erkläre ich, dass ich keine früheren Promotionsversuche unternommen habe.

München, 13.10.2005

Katrin Amann

Lebenslauf

Studium

Sept. 2002 – August 2005

Promotion am Botanischen Institut der LMU München bei Prof. Dr. R. G. Herrmann in der Arbeitsgruppe von PD Dr. J. Meurer

Arbeitsgebiet: *Assembly and Function of Photosystem I in Higher Plants*
Voraussichtlicher Abschluss der Promotion: Oktober 2005

Sept. 2004 – Feb. 2005

Forschungsaufenthalt mit einem Marie-Curie-Stipendium an der Royal Agricultural and Veterinary University in Kopenhagen bei Prof. Dr. H. V. Scheller

April 2001 – Dez. 2001

Diplomarbeit am Botanischen Institut der LMU München bei Prof. Dr. R. G. Herrmann in der Arbeitsgruppe von Dr. J. Meurer

Thema: *Genetische und molekulare Analyse einer selektierten T-DNA-induzierten Mutation von Arabidopsis thaliana*

Juni 2002 – März 2003

Hauptdiplomprüfung in Biologie
Note: mit Auszeichnung bestanden (Note: 1.0)
Hauptfach: Physiologische Botanik

Nov. 1996 – Juni 2002

Studium der Biologie und Biologie und Chemie für das Lehramt am Gymnasium an der LMU München
Abschluss: Staatsexamen (Note: 1,77)

Schulbildung

1987 – 1996

Besuch des Gymnasiums Miesbach
Abschluss: Allgemeine Hochschulreife (Note: 1,9)

1983 – 1987

Besuch der Grundschule Schliersee

München, Oktober 2005

Katrin Amann, *Dipl.-Biol.*, Stockholmstraße 13, 81829 München, Tel: (089) 30762376, katrinamann@web.de